AD _____

ALLEVIATION OF THE SIDE FORCE AND THE YAWING MOMENT ACTING ON A SLENDER CONE-CYLINDER BODY AT HIGH ANGLES OF ATTACK, USING SMALL JET INJECTION AT SUBSONIC AND TRANSONIC SPEEDS.

SECOND ANNUAL TECHNICAL REPORT

BY

D. ALMOSNINO and J. ROM

SEPTEMBER 1979.

EUROPEAN RESEARCH OFFICE
UNITED STATES ARMY
LONDON, ENGLAND

GRANT No. DAERO-78-G-119

DEPARTMENT OF AERONAUTICAL ENGINEERING
TECHNION - ISRAEL INSTITUTE OF TECHNOLOGY
HAIFA, ISRAEL.

UNCLASSIFIED

SECURITY CLASSIFICATION OF THIS PAGE (When Data Entered)

R&D 2416A

REPORT DOCUMENTATION PAGE

READ INSTRUCTIONS BEFORE COMPLETING FORM

1 REPORT NUMBER | 2 GOVT ACCESSION NO. | 3. RECIPIENT'S CATALOG NUMBER (9)

4. TITLE (and Subtitle)

Alleviation of the Side Force and the Yawing Moment Acting on a Slender Cone-Cylinder Body at High Angles of Attack, Using Small Jet Injection at Subsonic and Transonic Speeds.

5 TYPE OF REPORT & PERIOD COVERED

Second Annual Technical Report. 19 Sep 78— Sep 79

6. PERFORMING ORG. REPORT NUMBER

7. AUTHOR(s)

D. Almosnino and J. Rom

8. CONTRACT OR GRANT NUMBER(s)

DAERO-78-G-119?

9. PERFORMING ORGANIZATION NAME AND ADDRESS

Israel Institute of Technology
Dept. of Aeronautical Engineering
Technion, Haifa, Israel

10. PROGRAM ELEMENT, PROJECT, TASK AREA & WORK UNIT NUMBERS

6 11 02H
1T161102BH57-06

11 CONTROLLING OFFICE NAME AND ADDRESS

US Army Research & Standardization Group
Box 65, FPO NY 09510

12. REPORT DATE

Sep [redacted] 79

13. NUMBER OF PAGES

51

14. MONITORING AGENCY NAME & ADDRESS (if different from Controlling Office)

15. SECURITY CLASS. (of this report)

Unclassified

15a. DECLASSIFICATION/DOWNGRADING SCHEDULE

16. DISTRIBUTION STATEMENT (of this Report)

APPROVED FOR PUBLIC RELEASE

DISTRIBUTION UNLIMITED

17 DISTRIBUTION STATEMENT (of the abstract entered in Block 20, if different from Report)

18. SUPPLEMENTARY NOTES

19. KEY WORDS (Continue on reverse side if necessary and identify by block number)

20. ABSTRACT (Continue on reverse side if necessary and identify by block number)

The effects of small symmetrical jets of the side forces of slender bodies at high angles of attack are investigated. Control as well as alleviation of these forces are ~~under consideration~~. The effect of Reynolds number and blowing rate are investigated. Side force alleviation ~~has been~~ is obtained for subsonic and transonic flows. ~~The~~ variation of Mach number ~~effects~~ the magnitude and direction of ~~the~~ side forces.

DD FORM 1 JAN 73 1473 EDITION OF 1 NOV 65 IS OBSOLETE

UNCLASSIFIED

SECURITY CLASSIFICATION OF THIS PAGE (When Data Entered)

AD

ALLEVIATION OF THE SIDE FORCE AND THE YAWING MOMENT ACTING ON A SLENDER CONE-CYLINDER BODY AT HIGH ANGLES OF ATTACK, USING SMALL JET INJECTION AT SUBSONIC AND TRANSONIC SPEEDS.

SECOND ANNUAL TECHNICAL REPORT

BY

D. ALMOSNINO and J. ROM

SEPTEMBER 1979.

EUROPEAN RESEARCH OFFICE
UNITED STATES ARMY
LONDON, ENGLAND

GRANT No. DAERO-78-G-119

DEPARTMENT OF AERONAUTICAL ENGINEERING
TECHNION - ISRAEL INSTITUTE OF TECHNOLOGY
HAIFA, ISRAEL.

ABSTRACT

The research presented in this report is a further step in the investigation of the aerodynamic characteristics of slender bodies at high angles of attack, in subsonic and transonic Mach numbers, and it continues the research already done on the effect of small, symmetrical jet blowing from the nose of a cone-cylinder body on the alleviation and control of side forces and yawing moments at high angles of incidence.

In the present investigation the effects of Reynolds number, Mach number and the effect of varying the blowing rate are investigated. Strong effects on the transition of the boundary layer are found in the range of Reynolds numbers $0.6 \times 10^5 \div 0.8 \times 10^6$. Favourable results of side force control and alleviation are obtained when jet blowing is used together with a transition ring, at low subsonic speed. The experimental results, (including oil flow visualization) indicate that the jet injection affects both the transition of the boundary layer and also the stabilization of the symmetry of the vortex formation at low speed.

Side force alleviation has been obtained also at high subsonic and transonic Mach numbers, using a quite low blowing coefficient. Schlieren photographs indicate that in this case the effect of the blowing is to stabilize the separation of the vortices from the body, and seems also to inhibit the vortex breakdown.

The blowing becomes ineffective at the chosen station of injection, at $M > 0.85$, possibly because of the relative reduction in the blowing

rate coefficient and because of the shock waves which exist at these Mach numbers. The variation of Mach number is found to affect the magnitude of the side force and yawing moment, and more significantly their directions. However, the observed side forces and yawing moments are smaller in magnitude at high subsonic and trasonic Mach numbers in comparison with those obtained in laminar conditions at low speeds.

TABLE OF CONTENTS

LIST OF SYMBOLS

C_n	yawing moment coefficient, N/qSD
C_M	pitching moment coefficient, M/qSd
C_{NOR}	normal force coefficient, F_{NOR}/qS
C_Y	side force coefficient, Y/qS
C_μ	blowing rate coefficient, $\dot{m}_j u_j/qS$
D	reference chord (body diameter)
F_{NOR}	normal force to the body
$\dot{m}_j$	jet mass flow rate
M	Mach number
M, N	pitching and yawing moments (about nose tip point).
q	dynamic pressure, $\frac{1}{2}\rho V^2$
Re_D	Reynolds number, based on body diameter, $\frac{\rho VD}{\mu}$
S	reference area, (body cross section, $\frac{\pi D^2}{4}$)
u_j	theoretical jet velocity (assuming fully expanded isentropic flow)
V	freestream velocity
x	length measured from nose tip point, along body axis of revolution
Y	side force
α	angle of attack
ρ	air density
ϕ, θ	geometrical angles
μ	air viscosity

NOTE: All forces and moments are given in body axes of reference.

LIST OF FIGURES

FIGURE No.

LIST OF FIGURES (CONT'D)

1. INTRODUCTION

This report summarizes the research performed under Grant No. DAERO-78-G-119 during the period December 1st 1978 to August 31st 1979.

The interest in the performance at high angles of attack of missiles and aircraft is growing. Efforts are made to investigate the behaviour of slender and not so slender bodies at high angles of attack and to understand the phenomena related to the development of asymmetries in the separated vortex flow established about such bodies.

This asymmetry in the flow causes large side forces and yawing moments which act upon the body at zero side-slip angles. Therefore, efficient means of alleviating and controlling side-forces and yawing moments on such slender bodies at high angles of attack are investigated. The work presented here is an experimental investigation of the forces and moments acting on a cone-cylinder body at high angles of attack, in the subsonic and transonic speed ranges. This investigation includes the study of the effect of injection of small symmetrical air jets from the nose of the body and their effects on the lateral forces and moments.

This program is a continuation of the previous experimental work presented by Sharir, Portnoy and Rom [9], and also by Rom and Almosnino [10].

The investigation includes effects of Reynolds number and transition

strips, rate of jet blowing, and Mach number on the forces and moments acting on the body at high angles of attack, and it also includes some flow visualization tests which help to understand the influence of jet injection on the flow field close to the body surface.

2. LATERAL BEHAVIOUR OF SLENDER BODIES AT HIGH ANGLES OF ATTACK, AT SUBSONIC AND TRANSONIC SPEEDS.

Separation of the boundary layer occurs at moderate angle of attack because of the adverse cross flow pressure gradient on the leeward side of the slender body.

The separated boundary layer then rolls-up to form a system of distinct vortices. (The description of separation is more complicated when the body is not slender).

The rolled up vortex sheet may stay close to the body and be continuously fed from the separated boundary layer, or it may leave the body entirely further downstream. Separation line may be expected to be found near the line of minimum pressure coefficient on the leeward side of the body, since the separation is caused by the adverse pressure gradient [1].

Due to geometrical irregularities of the nose of the body and irregularities in the outer flow, one side of the boundary layer may separate first from the body, maintaining a certain vortex strength in the corresponding rolled-up vortex sheet. The other side of the boundary layer may remain attached and separate only further downstream on the body with a corresponding stronger vortex. In this manner the asymmetric vortex system is generated behind the body at high angles

of attack. This description is supported for example by results presented in Ref. 2 where it is shown that the side forces are associated with the asymmetry of circumferential pressure distribution and the asymmetry of the vortex sheet separation. Visualization presented in Ref. 1 show that the separation line is shifted towards the windward side of the body as the angle of incidence is increased. Measurement of the circumferential angles of separation indicate that asymmetry of the separation increases as the angle of incidence is increased (in laminar boundary layer conditions). The maximum angular difference nearly coincided with the maximum measured side force. (Maximum angular difference was of the order of 20^{o} to 40^{o} for sharp slender nose shapes). It was found in Refs. 1,2, and 3 that as the angle of attack was high enough, several vortex separations accured along the body.

The nose shape is a most significant parameter which affects the side forces. This is supported for example by results of Refs. 6,7, and 8. Refs. 23 and 29 for example show that reorientation of the nose about the body axis of revolution has a most considerable effect on the side force and yawing moment sign and magnitude. As it seems from the state of the art today, it is generally, accepted that the following phenomenological rules associated with flow asymmetry hold true:

(1) Initial direction of the side force or yawing moment is unpredictable because of its connection with small irregularities in nose geometry. However, once the direction is established, it does not change for given geometry and flow conditions.

Change of sign may occur as the angle of incidence is increased, (even more than once).

(2) Reynolds number has almost no effect on the angle of incidence for the onset of the asymmetry, but it has a notable effect on the magnitude of the side force.

(3) Magnitude of the side force increases with the increasing finess ratio of the nose.

(4) Side forces and yawing moments are very small below $\alpha = 25^{\circ}$. Beyond this they increase quite sharply and reach their peaks between 35° - 50°, depending on the Reynolds and Mach numbers and on the geometry of the configuration.

(5) Installing transition strips may cause reduction of the side force as much as 80%, causing early transition to turbulent boundary layer at low Reynolds numbers. (Surface roughness has also that kind of effect).

Several works try to give a model to predict the position of separation, the asymmetric vortex structure and the forces and moments acting on slender bodies at high angles of attack. (For example, Refs. 3,4,5, 11, 12, 13, 15, 16, 19, 20, 25, 30). As stated in Ref. 14, the success of these methods is only partial, and the theoretical state of the art for calculating steady asymmetric vortex patterns around bodies of revolution at low speeds is semi-empirical. At present only engineering methods of limited range of applicability are available.

Side forces and moments may be potentially hazardeous to the control and stability of slender configurations such as modern fighters

and missiles maneuvering at high angles of attack. These side forces and moments may be overcome by sufficient control authority, or by aerodynamic devices which suppress the asymmetric vortex pattern. The most common aerodynamic devices used for side force alleviation are transition strips of all kinds, and vortex generators such as small strakes usually placed on the forebody or near the nose.

In Ref. 6 reduction of side forces is achieved by adding meridianal strips of grit at angular positions $\theta = \pm 30^{\circ}$. In Ref. 7, the positioning of a ring on the nose caused a great reduction in the large yawing moments at high angles of attack. Ref. 8 shows that addition of vortex generators at the nose caused the separated vortices to be more symmetric at the critical angles of incidence.

Ref. 22 demonstrates the effectiveness of a pair of helical separation trips to disrupt the lee-side vortices, achieving great reduction of side forces and yawing moments. The effect of small strakes on reduction of side forces and yawing moments is demonstrated in Ref. 23.

It should be noted that the devices described above do suffer from certain defaults. Some of the transition strips used, reduced side forces but also had affected the normal force and pitching moment causing early "stall" effect. Strakes seem to be effective in alleviating side forces only in a certain limited range of angles of attack. In general, the role of these devices is a passive one, and apart from alleviating side forces, these devices could not be used for active lateral control of side forces and yawing moments at high angles of attack, for the benefit of improved maneuverability.

The present research continues the investigation on the effect of air jets blown from the nose of a body of revolution for the alleviation and also for the control of side forces and yawing moments at high angles of attack, in subsonic and transonic Mach numbers (previous results are reported in Refs. 9,10).

3. STUDIES OF SIDE FORCE AND YAWING MOMENT ALLEVIATION AND CONTROL ON A CONE-CYLINDER BODY AT HIGH ANGLES OF ATTACK, USING SMALL SYMMETRICAL JETS INJECTED FROM THE NOSE, AT SUBSONIC AND TRANSONIC MACH NUMBERS.

3.1. The model and the Experimental Facilities

The experiments are conducted in the Subsonic Wind Tunnel of the Aeronautical Research Center of the Technion with a cross section of 1m x 1m, and in the Transonic Wind Tunnel (blow down, induction type), with a cross section of 0.8m x 0.6m. The model shown in Fig. 1 is 3cm. dia. cylindrical body having an overall finess ratio of 6. The nose of the body is a pointed cone, with length/diameter ratio of 2. Using the results of previous experiments [9, 10], it was decided to concentrate the tests on a sharp cone forebody, and to inject the air jets from a station which was close to the nose apex at angles of - 30° to the horizontal plane of the body. This location of the pair of holes for injection gave the best results in the previous tests. The diameter of the holes was 1.2mm each, perpendicular to the body axis of revolution. (The diameter of the holes is chosen so as to obtain blowing velocities of the same order of magnitude as the tunnel flow speed).

A system of rigid and flexible tubing was arranged in the model so as to supply the air for symmetrical blowing. A special device

developed and built, which enabled continuous change of the rate of blowing and its measurement, so that the rate of blowing was directly recorded by the computer together with all other data readings during the experiments. Internal strain gage balances are used to measure the aerodynamic forces and moments. The balance chosen has particularly sensitive elements for the measurements of side forces and yawing moments. Visualization tests have been performed using oil-flow at low subsonic speeds and Schlieren photography at high subsonic and at transonic Mach numbers. Visualization tests have been carried out with and without injection, for comparison of the flow patterns. Tests with and without injection were repeated so as to verify the repeatability of the results.

Special measures were taken in the model installation to assure that the same angular position of the cone and the cylinder in each experiment is obtained in the tunnel so as to prevent any changes in the side force direction and magnitude due to variation in model installation.

The symmetry of the blowing jets is checked by blowing with no external flow and detecting zero lateral forces and moments.

3.2. Results

3.2.1. Low Subsonic Tests

The low subsonic tests are carried out at 32 m/sec. in an angle of attack range of -10° to 90°. Comparison is made between tests without a transition device, and tests with a transition strip (ring) of 0.1mm. thickness placed at $x/d = 0.333$ from the nose tip. (The thickness and

location of the transition ring are chosen according to Refs. 27, 28. The effect of the jet blowing is also tested with the without transition ring.

From Fig. 2 it can be seen that the normal force and pitching moment coefficients are only moderately affected by the transition ring especially near the region of their peak. Normal force peak with a transition ring is about 10-15% less than without transition, while there is only a slight difference between the curves up to 40^{o} angle of attack.

However, Figs. 3 and 4 show that the influence of the transition ring is quite large on the side force and yawing moment coefficients. There is a great reduction in the side force and yawing moment, using the transition ring, up to about 56^{o} angle of attack, while peak position for the side force being shifted down to about $\alpha = 41^{o}$ (from $\alpha = 48^{o}$ without the transition ring). The maximum side force coefficient is reduced by 25%, using the transition rings. It is also interesting to note the development of a negative secondary peak of side force , with the transition ring, at about $\alpha = 60^{o}$. Worth noting is also the fact that without the transition ring the maximum side force coefficient is at $\alpha = 48^{o}$, while the yawing moment peak is occuring at about $\alpha = 40^{o}$. The position of both these peaks occurs at about $\alpha = 41^{o}$ when the transition ring is present. The angle of onset of side forces is unaffected by the transition ring and stays at about 24^{o}.

Effects of Jet Injection on Side Forces and Yawing Moments, with and without Transition Ring.

The effect of jet injection is demonstrated in Figs. 5 and 6 (no

transition ring) and in Figs. 7 and 8 (with transition ring). In Figs. 5 and 6 it can be seen that jet blowing from the chosen station on the nose effectively alleviated side forces and yawing moments above $\alpha = 44^{o}$. Blowing is ineffective below $\alpha = 44^{o}$, without a transition ring.

The behaviour of the curve describing the variation of C_Y or C_n versus the blowing coefficient C_μ has a special form (when the blowing is effective). It can be seen that there is a sharp reduction in C_Y and C_n at a very low blowing rate, and as C_μ grows there is a change of sign, reaching a negative but lower peak (in absolute value). That peak is usually much more "flat" and when C_μ is increased further, a second zero of C_Y and C_n may be achieved, sometimes accompanied later by a second positive peak at high blowing rates. The very sharp change in C_Y and C_n at very low blowing rates might be caused by the jets, which act to trip the boundary layer. This possibility is supported by some oil flow visualization photographs, in which there is a distinct curved pattern starting from the injection holes, rolling up along the conical nose, up to the shoulder, or to the nearest separation lines. However, Figs.22,23 which are examples of the oil flow visualization photographs show that the small jets also affect the symmetry of the separation lines along the leeward side of the body. The effect of the jets on the boundary layer transition is clear also from their influence on C_{NOR} especially at high angles of incidence (Figs. 9, 10).

When a transition ring is present,(Figs. 7 and 8), the sharp change in C_Y and C_n disappears at $\alpha = 32^{o}$ and 36^{o}, and starts appearing again at $\alpha = 40^{o}$ up to about 58^{o}. This can be explained by the fact that the small transition ring is more effective at the lower

range of angles of attack in reducing sides forces, but it is less efficient at the higher angle of attack range, where the cross flow plane becomes more dominant, and there the effect of the jets is stronger.

Fig. 10 supports this view, where the normal force is unaffected by the jets at $\alpha = 32^{\circ}, 36^{\circ}$ with a transition ring, and starts being affected at higher angles of incidence.

The influence of injection apart from transitional effect is clearly demonstrated in Fig. 22 , where the transition ring is present, and the angle of incidence is 40°. Here the injection completely alters the separation pattern, apart from making it more symmetrical. The pair of separation lines on the leeside of the cone which continues over the shoulder along the cylinder without injection, breaks at the shoulder when injection is present,and a new pair of separation lines appears on the cylinder. The shoulder between the cone and the cylinder has been observed to have its own effects on the flow pattern, some of which are weaker or non-existent in models such as ogive-cylinder bodies. It should be noted that in the last case a higher blow rate was used for side force alleviation than in "transitional" cases (See Fig. 7 for $\alpha = 40^{\circ}$).

The amount of flow rate coefficient needed for side force alleviation vs. the angle of incidence is sketched in Fig. 11.

It is clear that high blowing rate is needed at the lower range of α , up to about $46^{\circ} \div 48^{\circ}$. Then there is the range of α(48° to 58° with transition ring, or 48° to 64° without it) where very low blowing

coefficient is needed to eliminate even high side forces. The last range corresponds to the negative slope region of C_Y vs. α, in general (Fig. 3).

The sharp rise in the required blowing coefficient at $\alpha = 60^o$, (with transition ring) corresponds with the negative peak of side force (Fig. 3), and the amount needed for side force alleviation is almost the same as was needed to alleviate the side force of the same positive amount at $\alpha = 40^o$. (The border lines which appear in Fig. 11 for some values of α are indicating the region of blowing rates in which side force is effectively zero or strongly alleviated).

3.2.2. High Subsonic and Transonic Speeds Tests

The effect of Mach number at two fixed angles of incidence, $\alpha = 46^o$, $\alpha = 48^o$, is shown in Figs. 12, 13. The rise in C_{NOR} and the equivalent change in C_M because of Mach number effect starts at about $M = 0.63$. It is interesting to see that both side force and yawing moment change their sign around $M = 0.7$, because of Mach number effects. (The reason might be connected with the first appearance of shock waves at that Mach number). The C_Y and C_n curves then reach an unstable peak between $M = 0.77$ and $M = 0.92$. This result is different from the conclusions presented in Ref. 14 which states that side forces on body of revolution are reduced to zero for crossflow Mach number greater than about 0.5.

It can be seen (Fig. 13) that there is a great reduction in the side force and yawing moment when the Mach number exceeds $M = 0.92$. (Equivalent cross flow Mach number is about 0.66).

Fig. 24 shows the development of the flow as the Mach number grows from 0,4 to 1.1, using Schlieren photographs.

The variation of C_Y and C_n vs. the angle of incidence at various Mach numbers is shown in Figs. 14, 15. Noteworthy is the sharp change in C_Y and C_n at $M = 0.4$, from a mild positive peak to a sharp negative peak, and then again to a mild positive peak. The reason might be connected with vortex breakdown. In general, the side forces and yawing moments above $M = 0.4$ are about 4 or 5 times less than at $M = 0.1$, and the reason is that the flow becomes fully turbulent, together with possible vortex breakdown phenomenon. (See also discussion of Reynolds number effect).

The Effect of Jet Blowing at High Subsonic and Transonic Mach Numbers.

The effect of jet blowing on C_Y and C_n is presented in Figs. 16 to 18.

The rates of jet blowing coefficient became quite small as the Mach number increased, so its effect is only partial.

At $M = 0.4$ (Fig. 16) jet blowing is ineffective at $\alpha = 46^o$ and causes an unstable change in C_Y and C_n at $\alpha = 48.5^o$. This is explained by results shown in Figs. 14, 15, where a sharp slope in C_Y and C_n is observed in this region.

At $M = 0.7$ (Fig. 17) there is a considerable alleviation of C_Y and C_n at $\alpha = 37.5^o$, but the blowing caused higher C_Y and C_n at $\alpha = 46^o$, where the side force is initially close to zero.

Schlieren photographs taken at $\alpha = 37.5^o$ and at that Mach number

with and without injection reveal some information about the effect of jet blowing in this case. It can be clearly seen in Fig. 25 that the main nose separated vortex line is broken near the shoulder of the cone without injection, (possibly because of the small shock line starting at this point). Secondary separations are observed further on the cylindrical part. However, with the blowing it can be seen that a distinct vortex is separated from the nose, trailing high above the cylindrical part and not broken in the shoulder region. Secondary separations are still observed on the cylinder.

At M = 0.85 (Fig. 18), jet blowing at $\alpha = 47^{o}$ managed to alleviate C_Y, but only reduced C_n. No effect of jet blowing at this rate is noted at M = 1.70.

One also should remember that at transonic Mach numbers, where shock waves are involved, there might be a stronger importance to the position of the jet blowing stations.

The effect of the small rate of jet blowing at transonic and high subsonic Mach numbers is noteworthy (when existent). Clearly the effect is not due to transition of the boundary layer because of the already high Reynolds numbers, and tunnel noise level. The Schlieren photograph of Fig. 25 clearly reveals that it has to do with vortex separation and breakdown. (The fact that jets can inhibit vortex breakdown is already known).

3.2.3. Reynolds Number Effect

Fig. 19 shows the effect of Reynolds number on C_{NOR} and C_Y, at various angles of attack. It is clear that there is a strong

transition effect of Re_D on these forces, at all angles of attack, causing a sharp drop in C_{NOR} at the higher Reynolds numbers which explains the lower C_{NOR} for a given α at $M = 0.4$, compared to the $M = 0.1$ results. At higher angles of incidence the variation of the C_{NOR} is somewhat similar to the variation of the drag coefficient (and indeed at those angles a large portion of the C_{NOR} is due to the drag). The behaviour of C_Y is very interesting.

It is clear that there is a sharp change of sign in C_Y in the transitional region, and then a more moderate rise, changing sign again at a higher Re_D. These results show clearly that the direction of sideforce might be changed because of Reynolds number effects in the transition region. Therefore under such conditions the side force may not stay in its original direction as some investigators suggested. (in this connection see also Refs. 17, 21 and 25).

Figs. 20 and 21 show the effect of Reynolds number on the pitching moment and on the yawing moment coefficients. The variation in the pitching and yawing moments at various Reynolds numbers indicate that unstable behaviour of the model may occur at high angles of attack, requiring special attention in the control considerations of these designs at certain ranges of speeds and altitudes. In view of these phenomena, blowing of jets may be a useful method for stabilization and controlling at such flight conditions.

3.3. Conclusions

The experimental investigation performed on the cone-cylinder body revealed important features of such configurations at high

angles of attack, and their dependence on Mach number and Reynolds number.

At least some of the so called uncertainties in the prediction of the general behaviour of side forces and yawing moments are found to be clearly dependent on these parameters. The strong effect of jet blowing on latteral forces and moments at various Mach numbers and Reynolds numbers has been demonstrated. At low subsonic speed, jet blowing at the chosen station may be used efficiently for side force alleviation and even control, especially when a transition ring is present also. Jet blowing at small rates is sufficient to alleviate side forces in some cases at high subsonic and transonic Mach numbers, but the rate required for controlling these forces must be much larger. Further experiments are needed at the transonic range in order to investigate the effects of parameters such as higher blowing rates and the effects of changes in the blowing stations. More visualization tests can also be useful in order to understand better the various roles of jet injection, in alleviating side forces and yawing moments.

REFERENCES

1. Pick, G.S., Investigation of side forces on ogive cylinder bodies at high angles of attack in the M = 0.5 to 1.1 range , AIAA Paper No. 71-570, June 1971.

2. Krouse, J.R., Induced side forces on slender bodies at angles of attack and Mach numbers of 0.55 - 0.80, NSRDC Test Rept. May 1971.

3. Thomson, K.D., and Morrison, D.F., The spacing position and strength of vortices in the wake of slender cylindrical bodies at large incidence, Weapons Research Establishment, Salisbury, South Australia, Tech. Rept. NSA 25, June 1969, (also Jr. of Fluid Mech., Vol. 50, Pt. 4, Dec. 1971, pp.751-783).

4. Lamont, P.J., and Hunt, B.L., Pressure and force distribution on a sharp-nosed circular cylinder at large angles of inclination to a uniform subsonic stream, Jr. of Fluid Mechanics, Vol. 76, Pt. 3, pp. 519-559, Aug. 1976.

5. Lamont P.J., and Hunt, B.L., Prediction of aerodynamic out of plane forces on ogive-nosed circular cylinders, Jr. of Spacecraft and Rockets, Vol. 14, No. 1, Jan. 1977, pp. 31-44.

6. Keener, E.R., and Chapman, G.T., Onset of aerodynamic side forces at zero sideslip on symmetric forebodies at high angles of attack, AIAA Paper 74-770, Aug. 1974.

7. Letko, W., A low speed experimental study of directional characteristics of sharp-nosed fuselage through a large angle of attack range at zero angle of sideslip, NACA TN 2911, March 1953.

8. Clark, W.H., Peoples, J.R., and Briggs, M.M., Occurence and inhibition of large yawing moments during high incidence flight of slender missile configurations, AIAA Paper No. 72-968, Sept. 1972.

9. Sharir, D., Portnoy, H., and Rom, J., "A Study of the effects of jets injected from a slender body of revolution on the side forces acting on it at large angles of attack in low speeds, TAE Rept. 337, May 1978, Technion, Israel Inst. of Technology.

10. Rom, J., and Almosnino, D., Studies of Non-linear aerodynamic characteristics of finned slender bodies at high angles of attack, TAE Rept. No. 349, Nov., 1978, Technion,Israel Inst. of Technology.

11. Fidler, J.E.,Approximate method for estimating wake vortex strength, AIAA Jr. Vol. 12, No. 5, May 1974.

12. Marshall, F.J., and Deffenbaugh, F.D., Separated flow over bodies of revolution using an unsteady discrete vorticity cross wake, NASA CR 2414, June 1974.

13. Mendenhall, M.R., and Nielsen, J.N., Effect of symmetrical vortex shedding on the longitudinal aerodynamic characteristics of wing-body-tail combinations, NASA CR 2473, Jan. 1975.

14. Nielsen, J.N., Nonlinearities in missile aerodynamics, AIAA Paper No. 78-20, Jan. 1978.

15. Angelucci, S.B., A multi vortex method for axisymmetric bodies at angles of attack, Jr. of Aircraft, Vol. 8, No. 12, 1971, pp 959-966.

16. Angelucci, S.B., Multi vortex model for bodies of arbitrary cross sectional shapes, AIAA Paper No. 73-104, 1973.

17. Clark, W.H., and Nelson, R.C., Body vortex formation on missiles at high angles of attack, AIAA Paper No. 76-65, Jan. 1976.

18. Clark, W.H., Body vortex formation on missiles in incompressible flows, AIAA Paper No. 77-1154, Aug. 1977.

19. Deffenbaugh, F.D., and Koerner, W.G., Asymmetric wake development and associated side force on missiles at high angles of attack, AIAA Paper No. 76-364, July 1976.

20. Smith, J.H.B., Inviscid fluid models, based on rolled-up vortex sheets, for three dimensional separation at high Reynolds number, RAE TECH. MEMO. AERO 1738, Nov. 1977.

21. Przirembel, C.E.G., and Shereda, D.E., Aerodynamics of slender bodies at high angles of attack", Jr. of Spacecraft and Rockets, Vol. 16, No. 1, Jan-Feb, 1979.

22. Rao, D.M , Side-Force alleviation on slender, pointed forebodies at high angles of attack, AIAA Paper No. 78-1339, 1978.

23. Coe, P.L., Chambers, J.R., and Letko, W., Asymmetric lateral-directional characteristics of pointed bodies of revolution at high angles of attack, NASA TN D-7095, Nov. 1972.

24. Clarkson, M.H., Malcolm, G.N., and Chapman, G.T., "A Subsonic, high-angle-of-attack flow investigation at several Reynolds numbers, AIAA Jr., Vol. 16, No. 1, Jan. 1978.

25. Redding, P.J., and Ericsson, L.E., Maximum vortex-induce side force, Jr. of Spacecraft and Rockets, Vol. 15, No. 4, July-Aug. 1978.

26. Schwind, R.G., and Mullen, J. Jr., "Laser Velocimeter measurements of slender body wake vortices, AIAA Paper No. 79-0302, Jan. 1979.

27. Braslow, A.L., and Knox E.C., Simplified method for determination of critical height of distributed roughness particles for boundary-layer transition at Mach numbers from 0 to 5, NACA TN 4363,1958.

28. Stewart, D.G., and Fisher, S.A., "Some observations of boundary layer transition on cones at subsonic and supersonic speeds, ARL Note ME 267, 1965.

29. Keener, E.P., Chapman, G.T., Cohen, L., and Taleghani, J., Side forces on a tangent ogive forebody with a finess ratio of 3.5 at high angles of attack and Mach numbers from 0.1 to 0.7, NASA TMX-3437, Feb. 1977.

30. Wardlaw, A.B., Jr., Multivortex model of asymmetric shedding on slender bodies at high angle of attack, AIAA Paper No. 75-123, Jan. 1975.

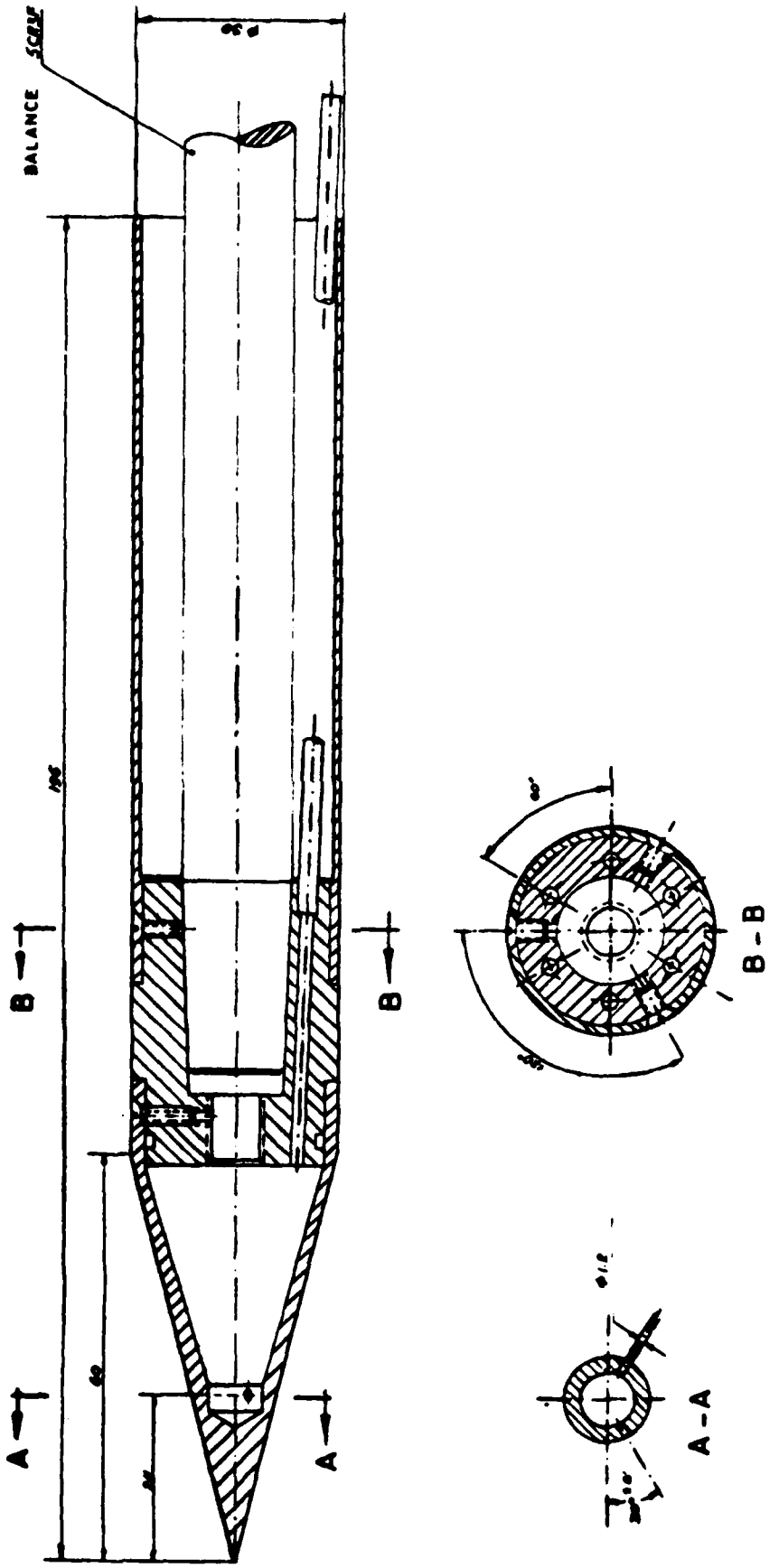

FIGURE No. 1 - THE CONE-CYLINDER MODEL.

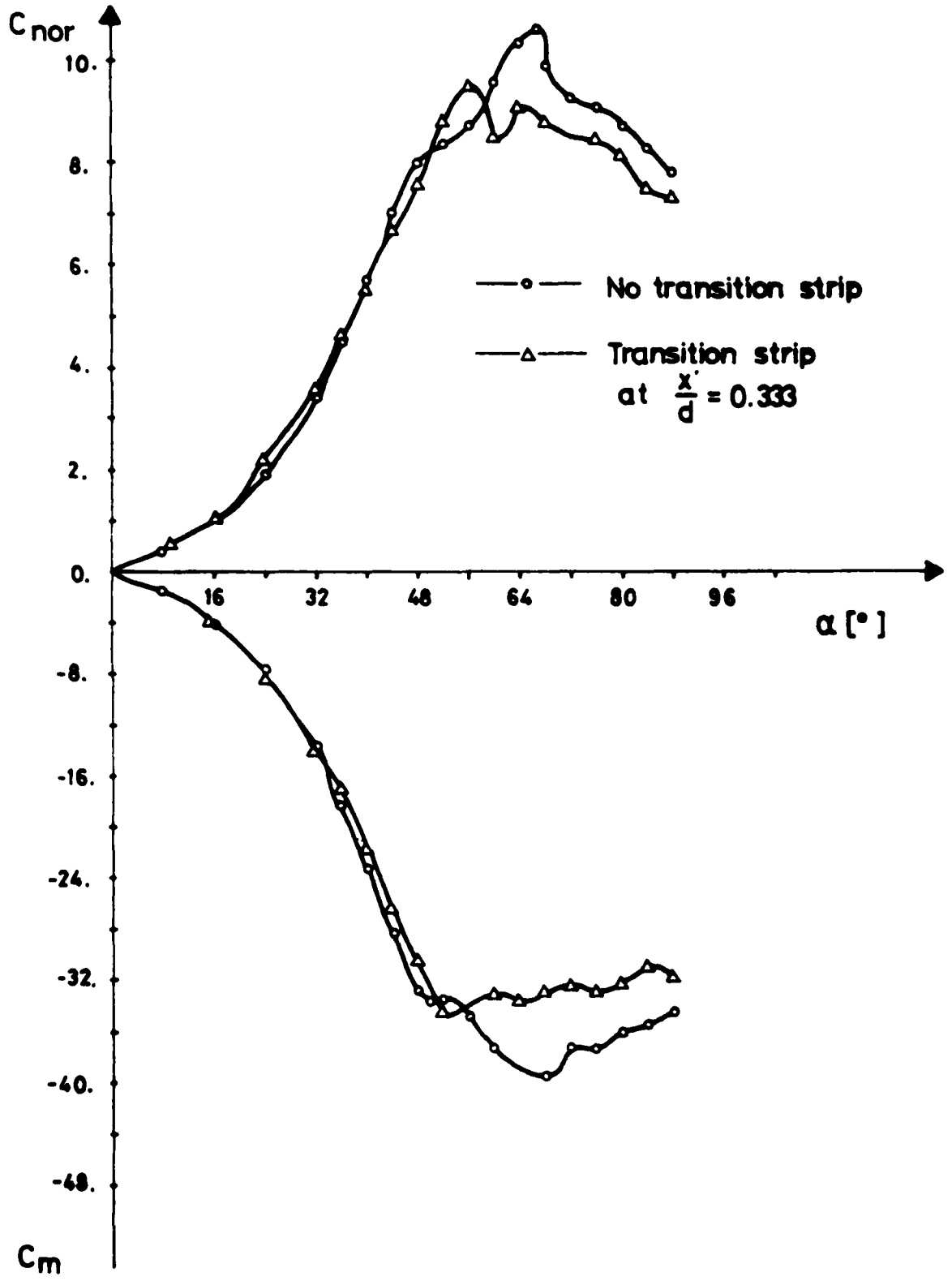

FIGURE No. 2 - NORMAL FORCE AND PITCHING MOMENT COEFFICIENTS Vs. ANGLE OF ATTACK, V = 32 m/sec, NO INJECTION.

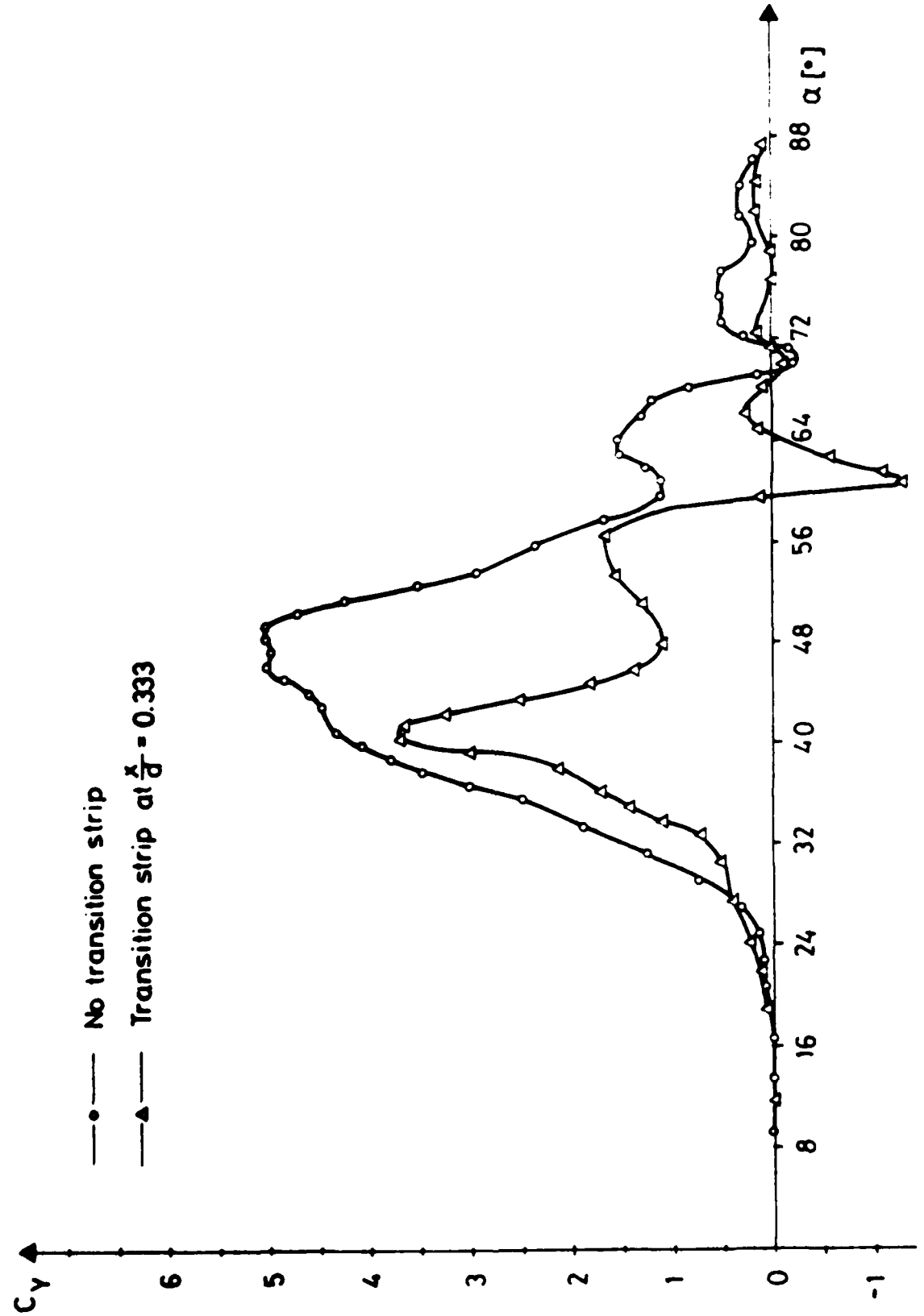

FIGURE No. 3 - SIDE FORCE COEFFICIENT Vs. ANGLE OF ATTACK, V = 32 m/sec, NO INJECTION.

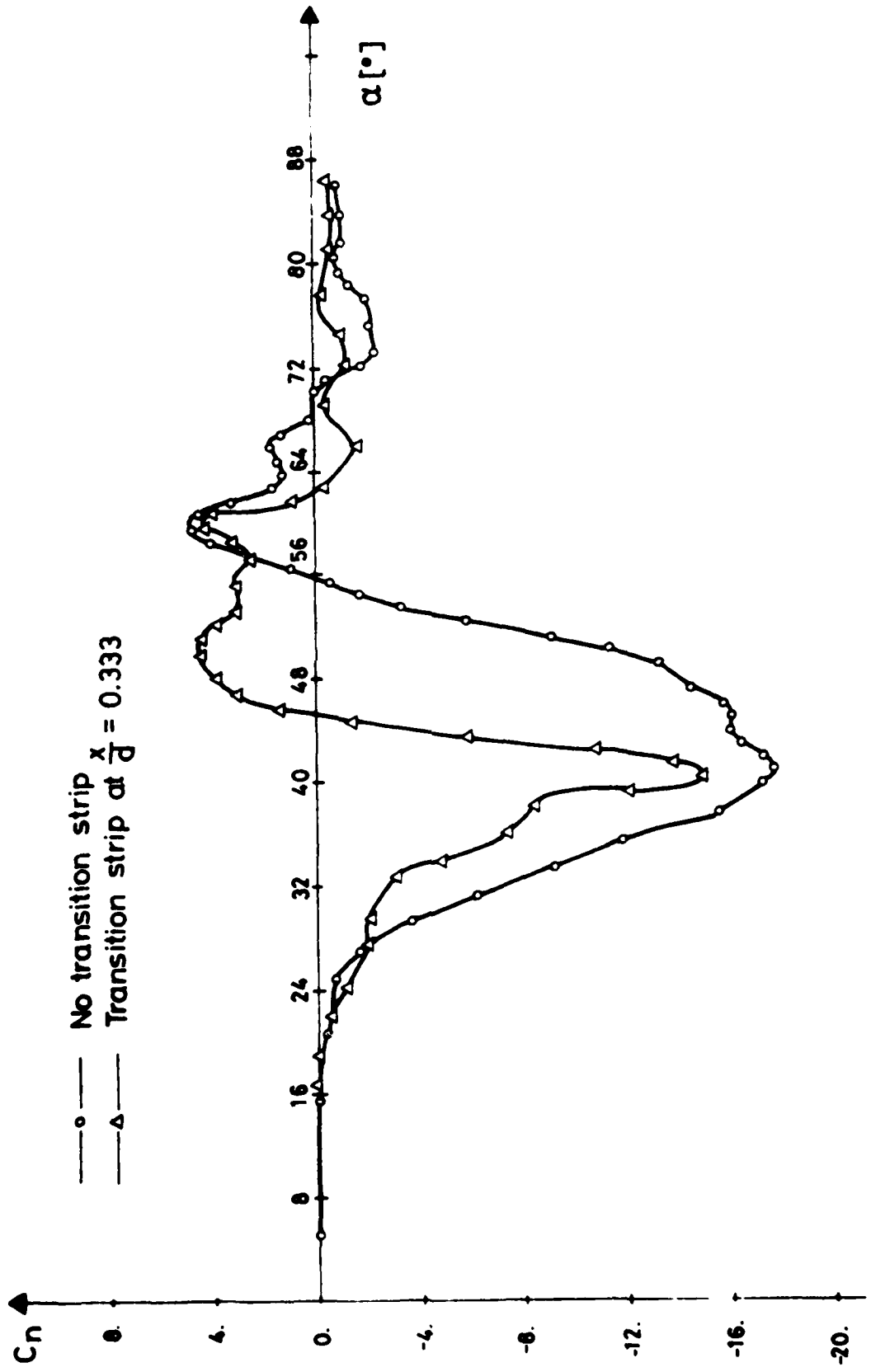

FIGURE No. 4 - YAWING MOMENT COEFFICIENT Vs. ANGLE OF ATTACK, V = 32 m/sec, NO INJECTION.

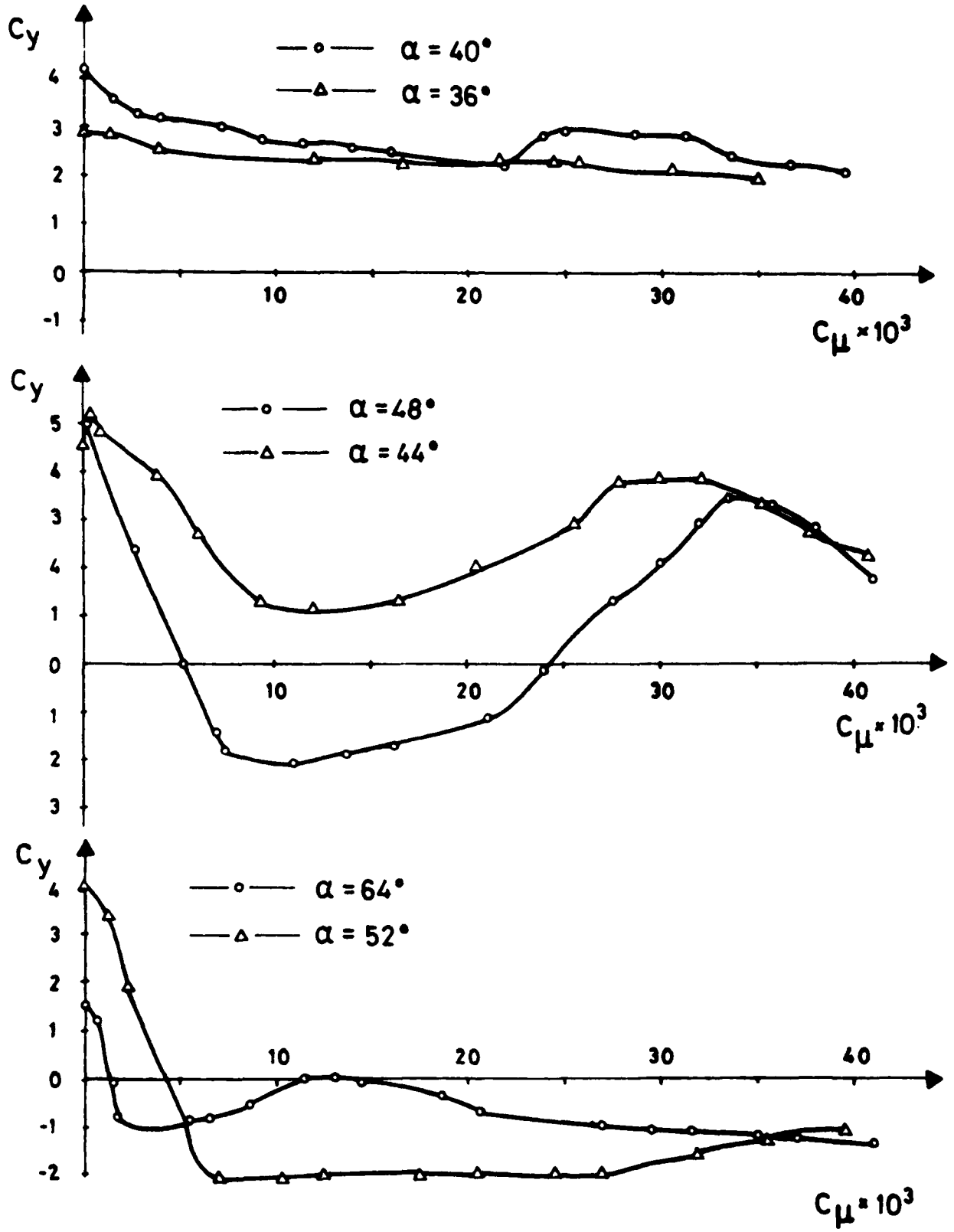

FIGURE No. 5 - VARIATION OF SIDE FORCE COEFFICIENT Vs. BLOWING RATE COEFFICIENT, AT VARIOUS ANGLES OF ATTACK, V = 32 m/sec, NO TRANSITION STRIP.

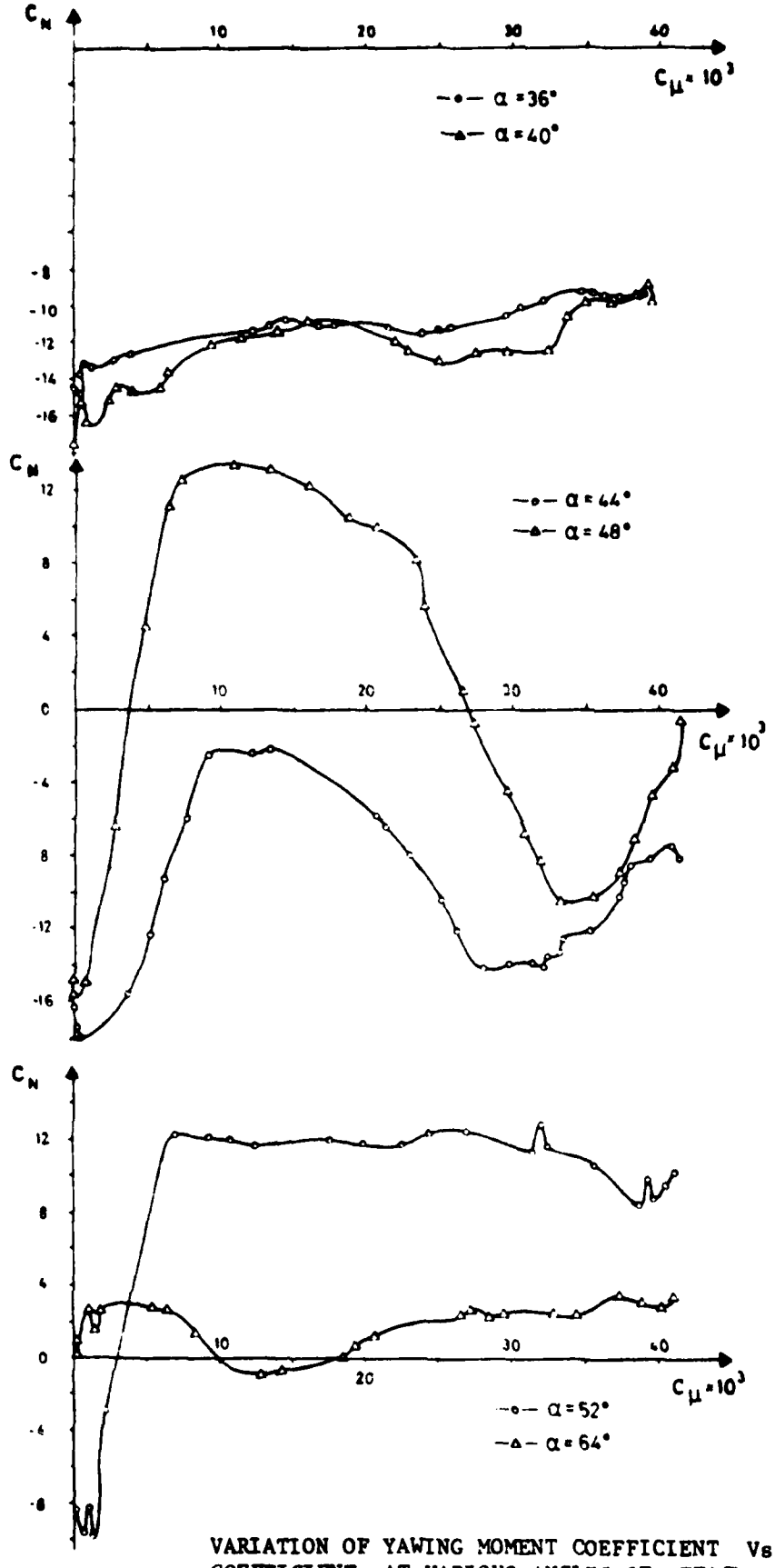

FIGURE No. 6 - VARIATION OF YAWING MOMENT COEFFICIENT Vs. BLOWING RATE COEFFICIENT, AT VARIOUS ANGLES OF ATTACK, V = 32 m/sec, NO TRANSITION STRIP.

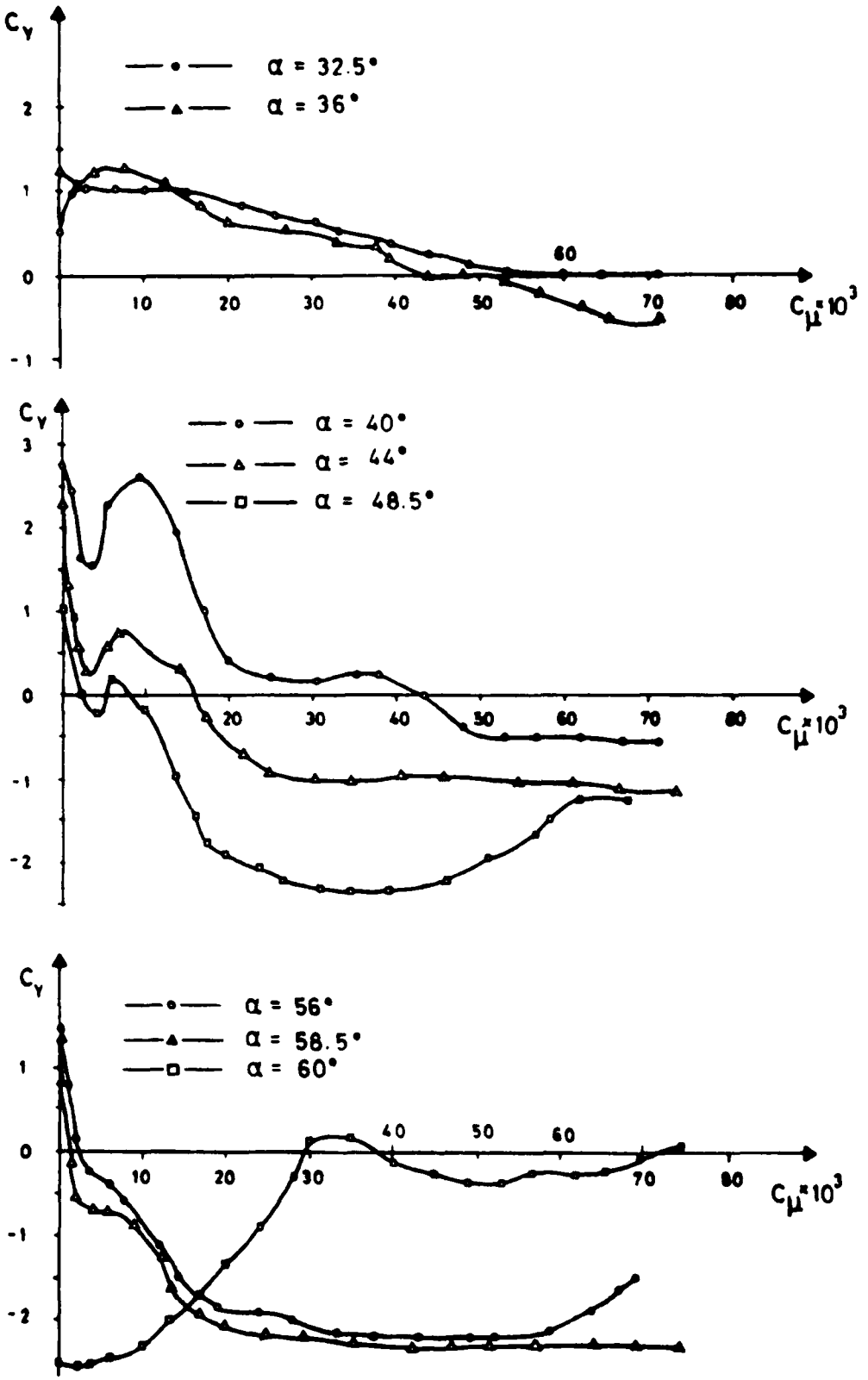

FIGURE No. 7 - VARIATION OF SIDE FORCE COEFFICIENT Vs. BLOWING RATE COEFFICIENT, AT VARIOUS ANGLES OF ATTACK, V = 32 m/sec, WITH TRANSITION STRIP at $\pi/d = 0.333$.

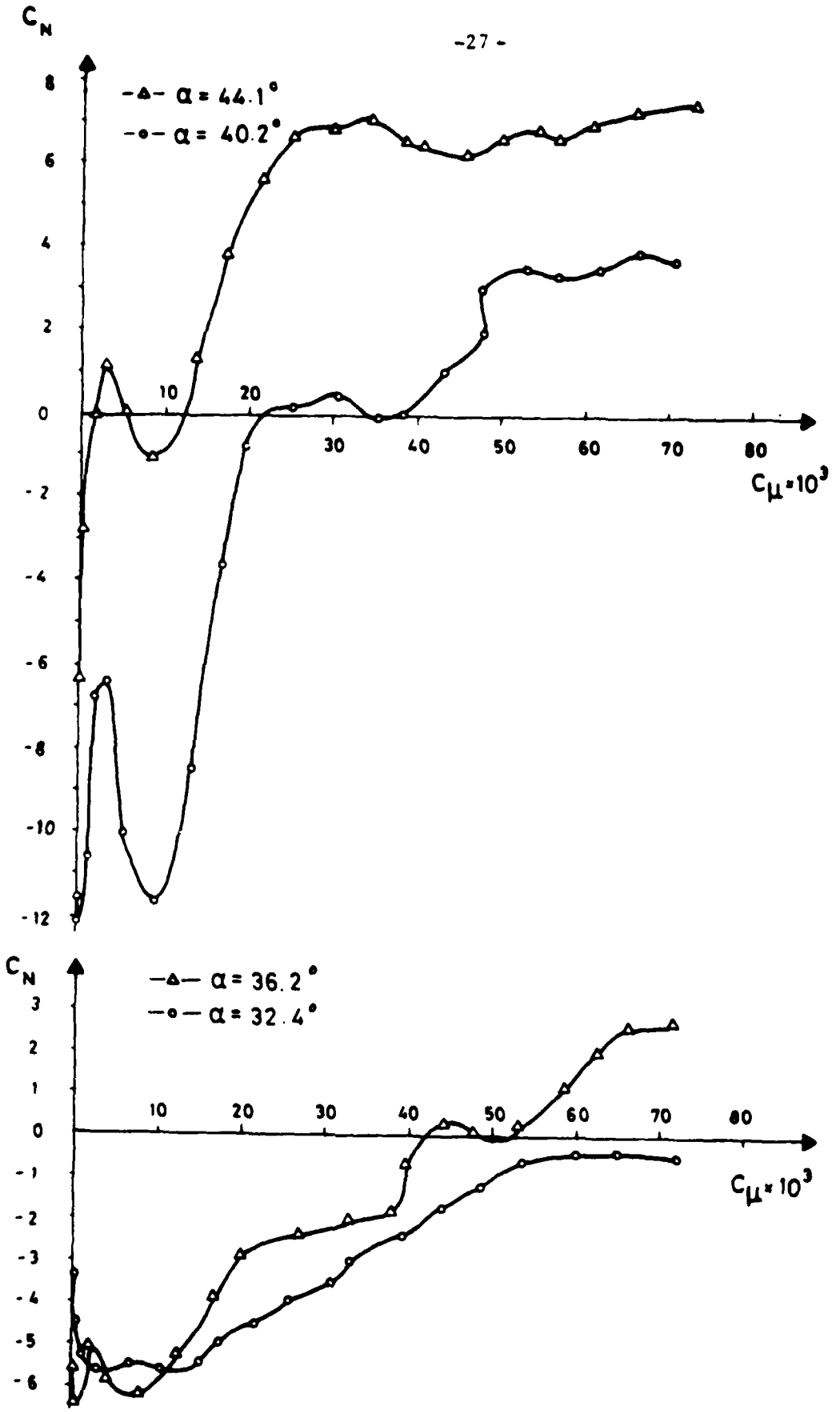

FIGURE No. 8 - VARIATION OF YAWING MOMENT COEFFICIENT Vs. BLOWING RATE COEFFICIENT, AT VARIOUS ANGLES OF ATTACK, V = 32 m/sec, WITH TRANSITION STRIP AT x/d = 0.333.

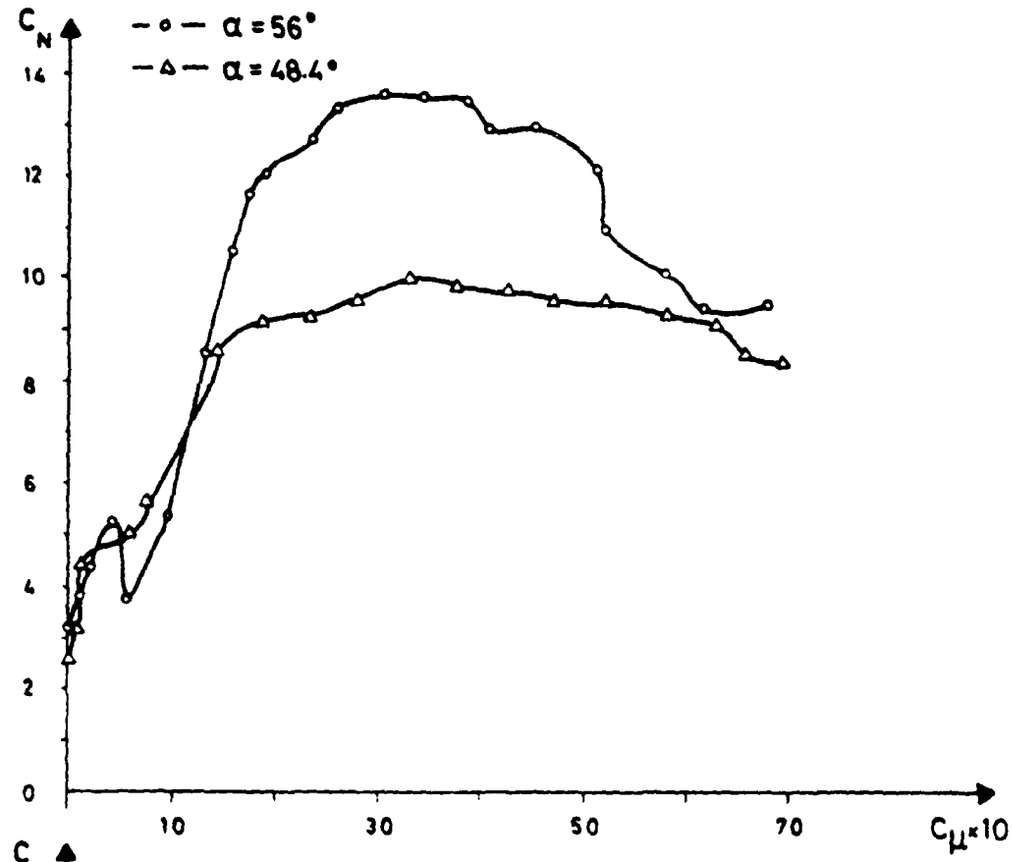

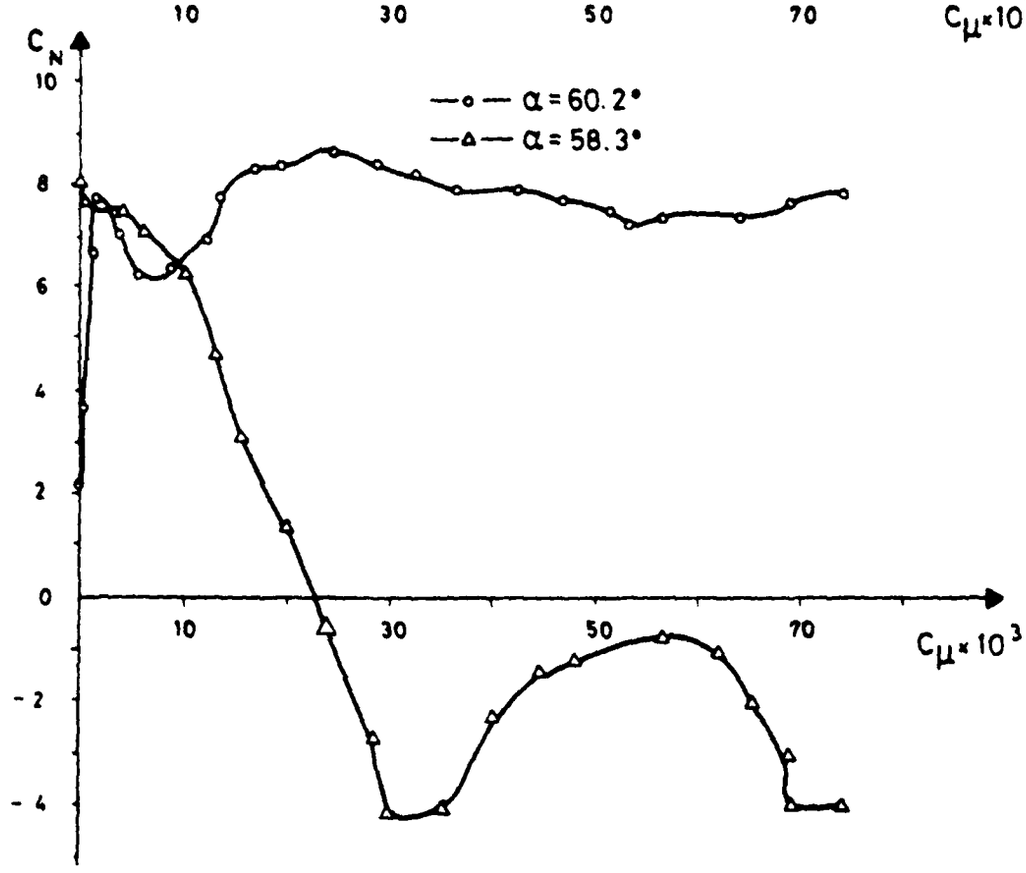

FIGURE No. 8 - CONTINUED

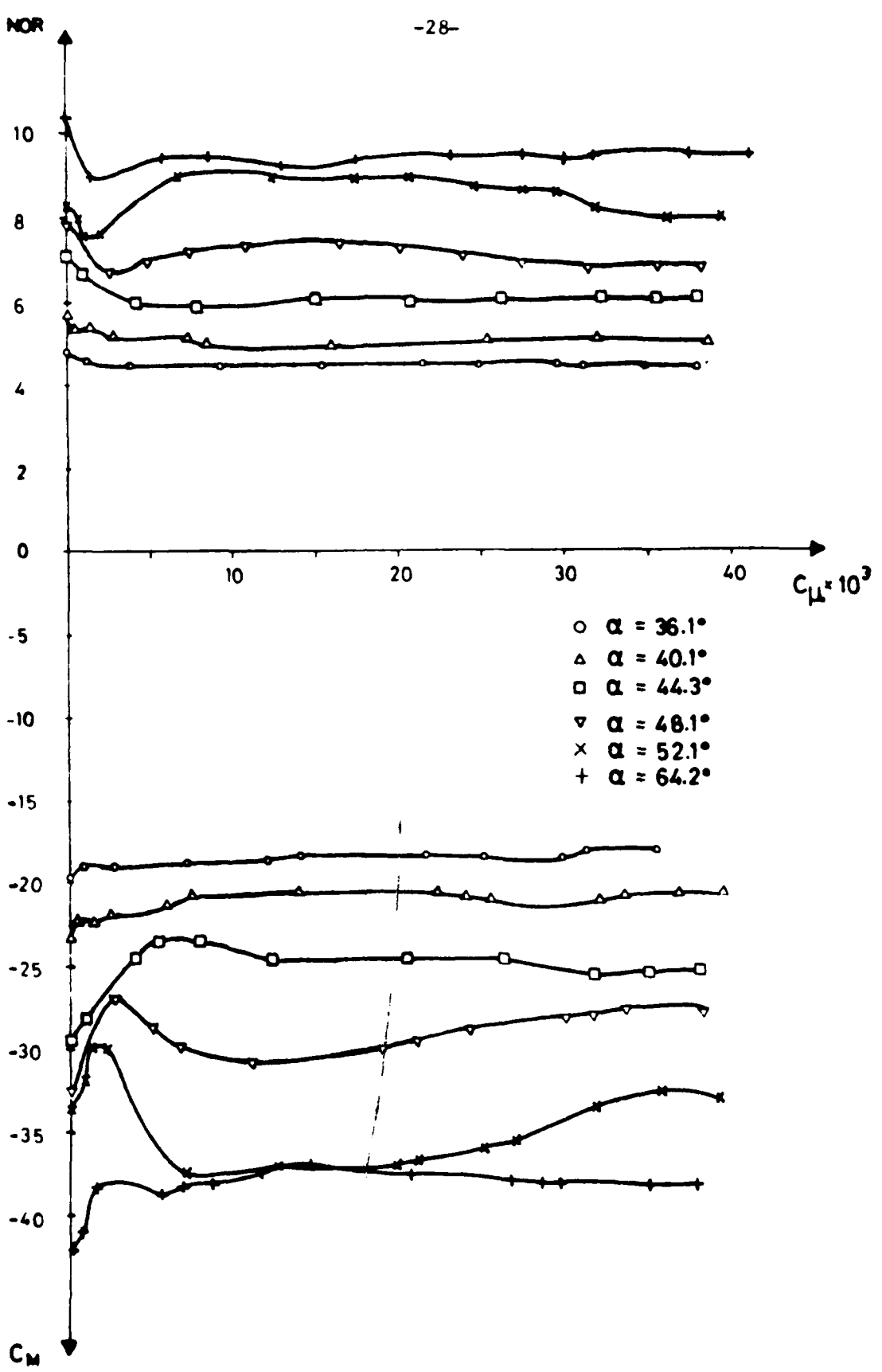

FIGURE No. 9 - NORMAL FORCE COEFFICIENT AND PITCHING MOMENT COEFFICIENT Vs. BLOWING RATE COEFFICIENT, AT VARIOUS ANGLES OF ATTACK, V = 32 m/sec, NO TRANSITION STRIP.

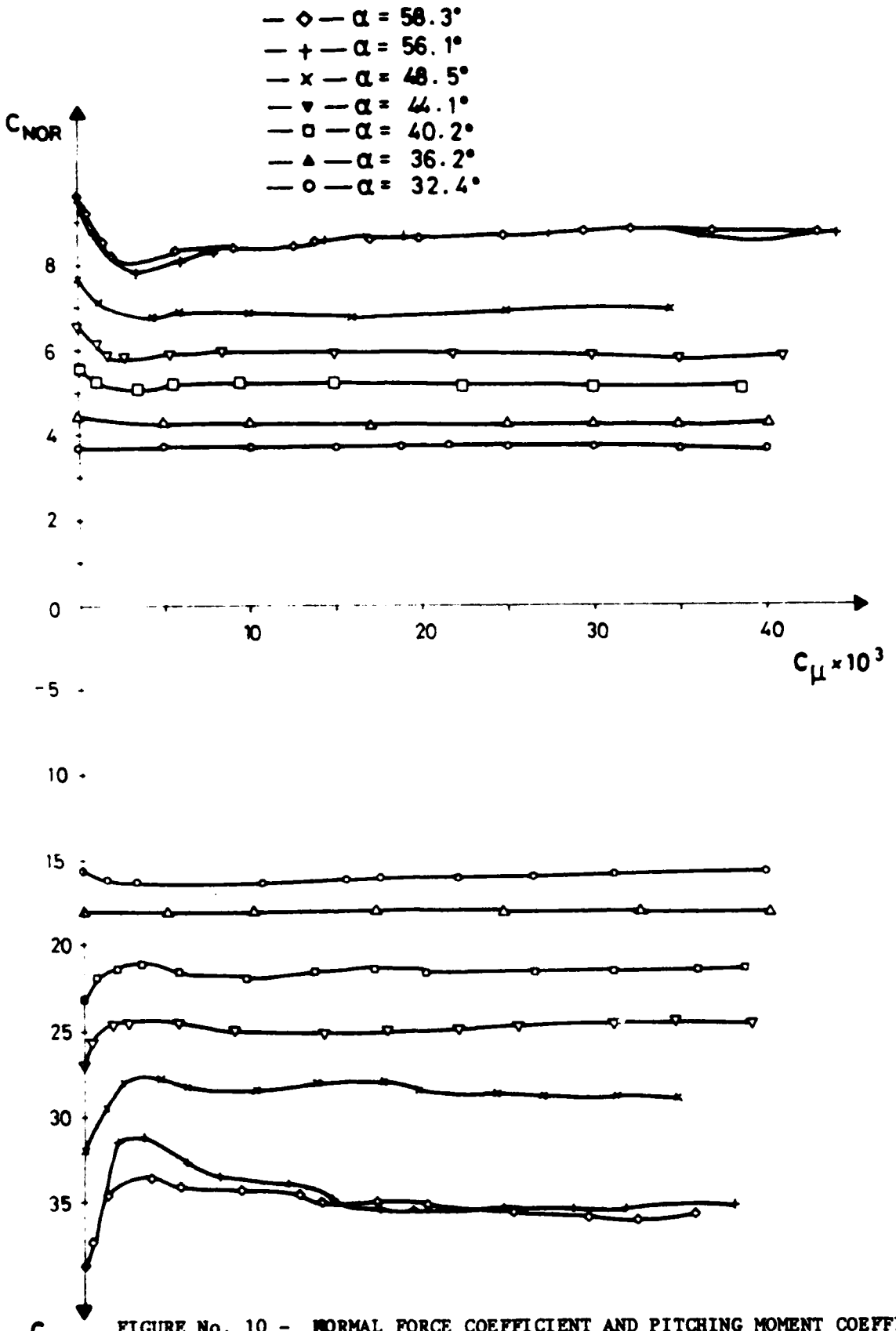

FIGURE No. 10 - NORMAL FORCE COEFFICIENT AND PITCHING MOMENT COEFFICIENT Vs. BLOWING RATE COEFFICIENT, AT VARIOUS ANGLES OF ATTACK, V = 32 m/sec, WITH TRANSITION STRIP AT x/d = 0.333.

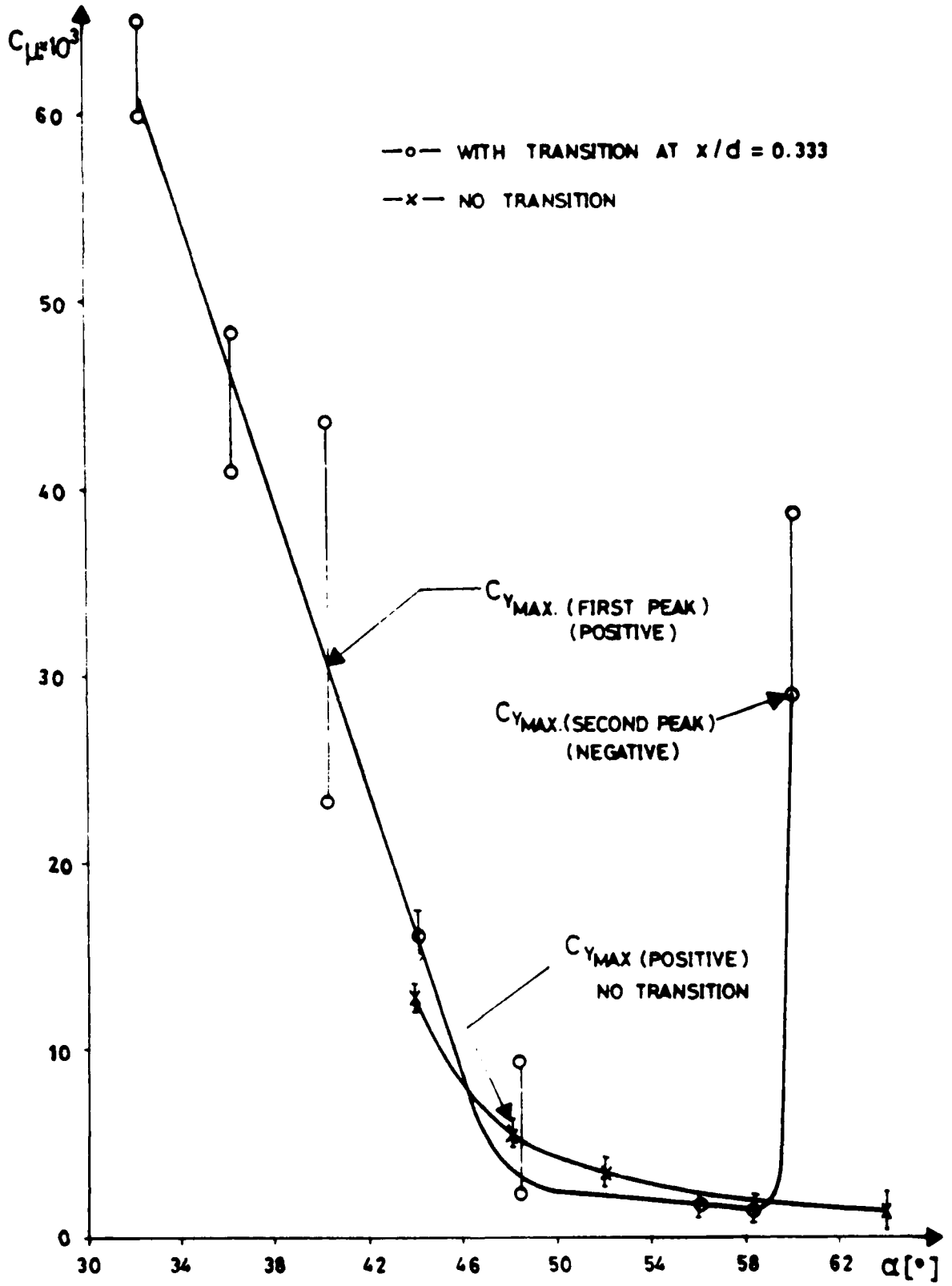

FIGURE No. 11 - BLOWING RATE COEFFICIENT NEEDED FOR SIDE FORCE ALLEVIATION AT VARIOUS ANGLES OF ATTACK.

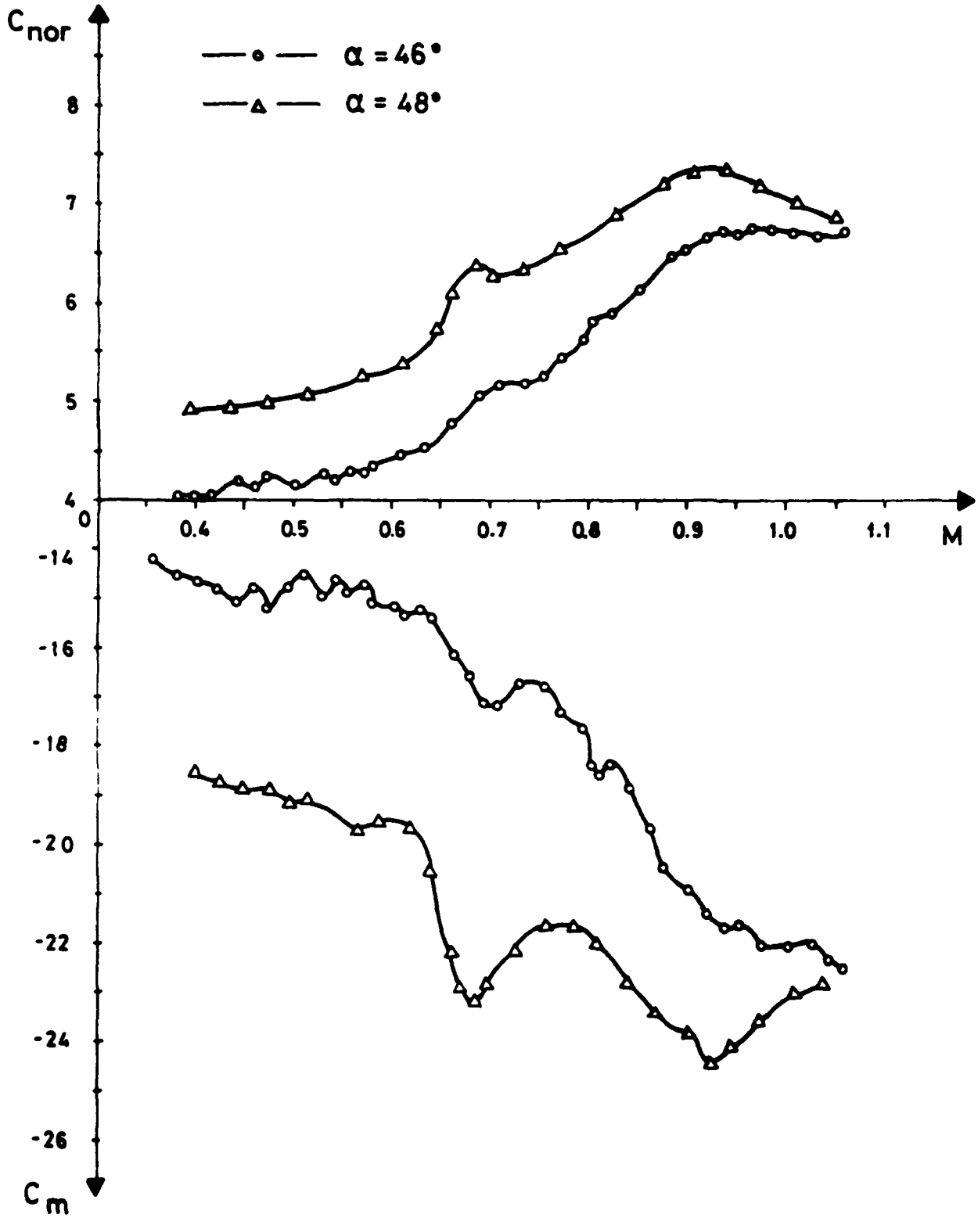

FIGURE No. 12 - NORMAL FORCE AND PITCHING MOMENT COEFFICIENTS Vs MACH NUMBER, AT TWO ANGLES OF ATTACK, NO TRANSITION STRIP, NO INJECTION.

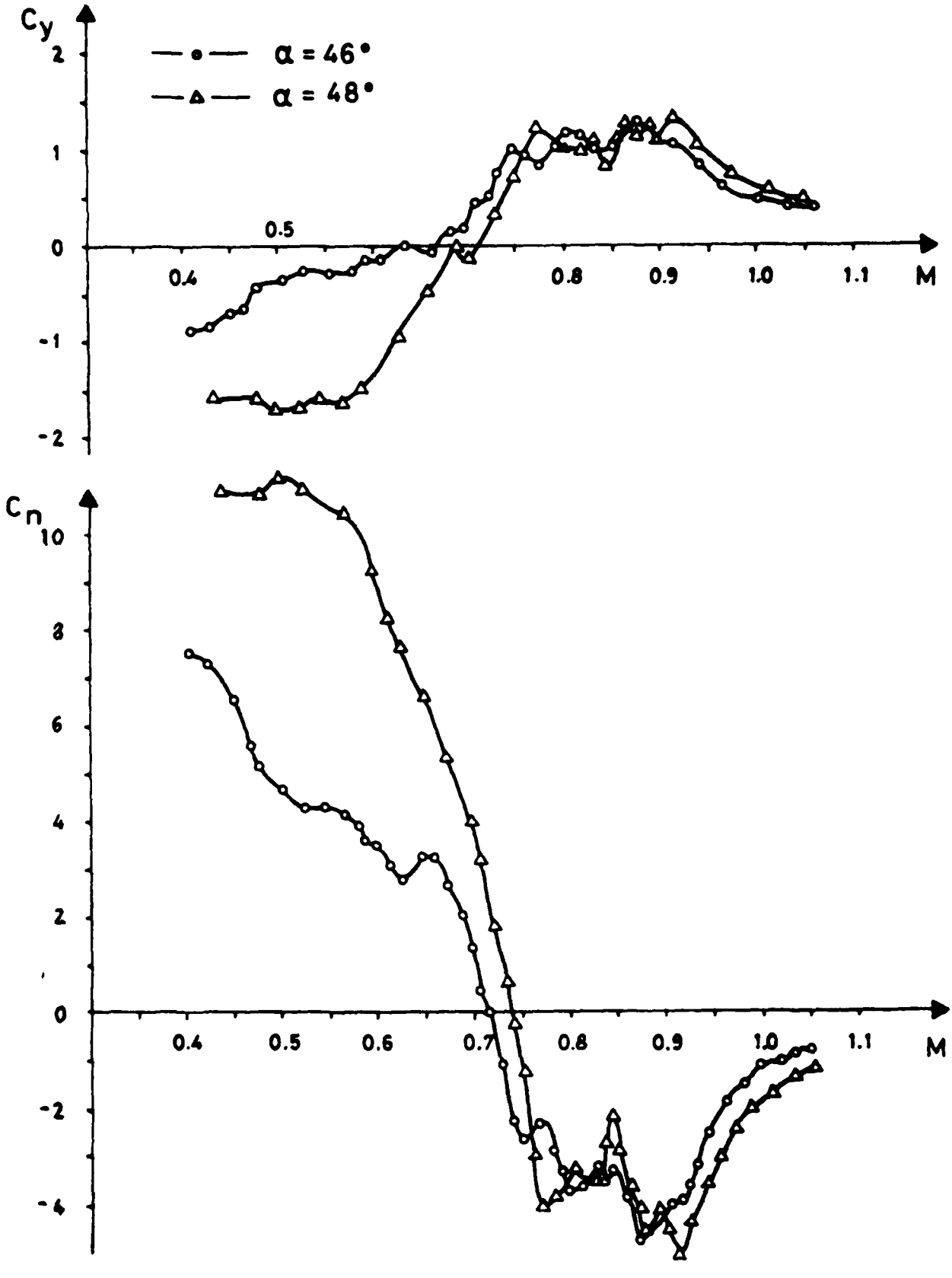

FIGURE No. 13 - SIDE FORCE AND YAWING MOMENT COEFFICIENT Vs. MACH NUMBER, AT TWO ANGLES OF ATTACK, NO TRANSITION STRIP, NO INJECTION.

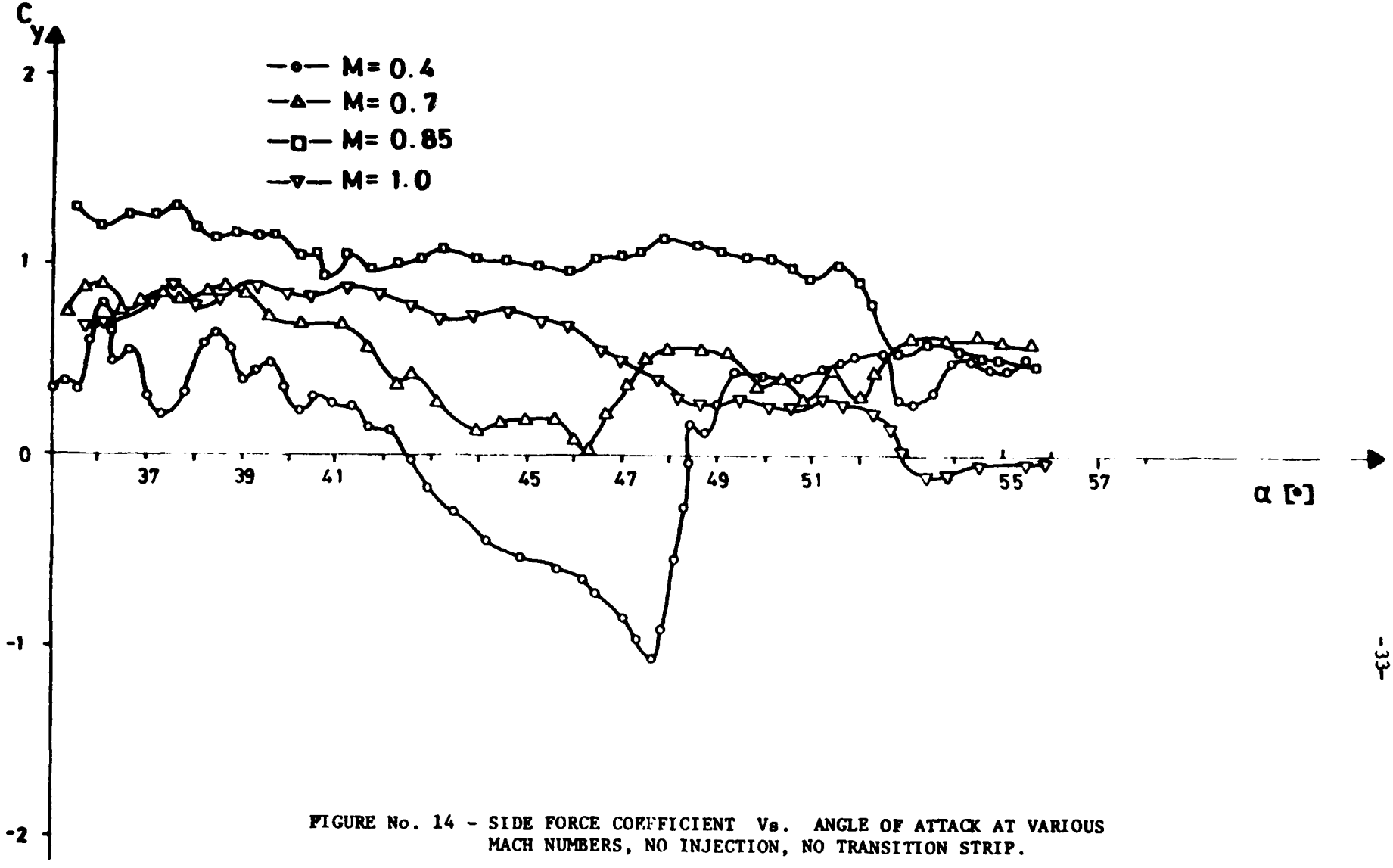

FIGURE No. 14 - SIDE FORCE COEFFICIENT Vs. ANGLE OF ATTACK AT VARIOUS MACH NUMBERS, NO INJECTION, NO TRANSITION STRIP.

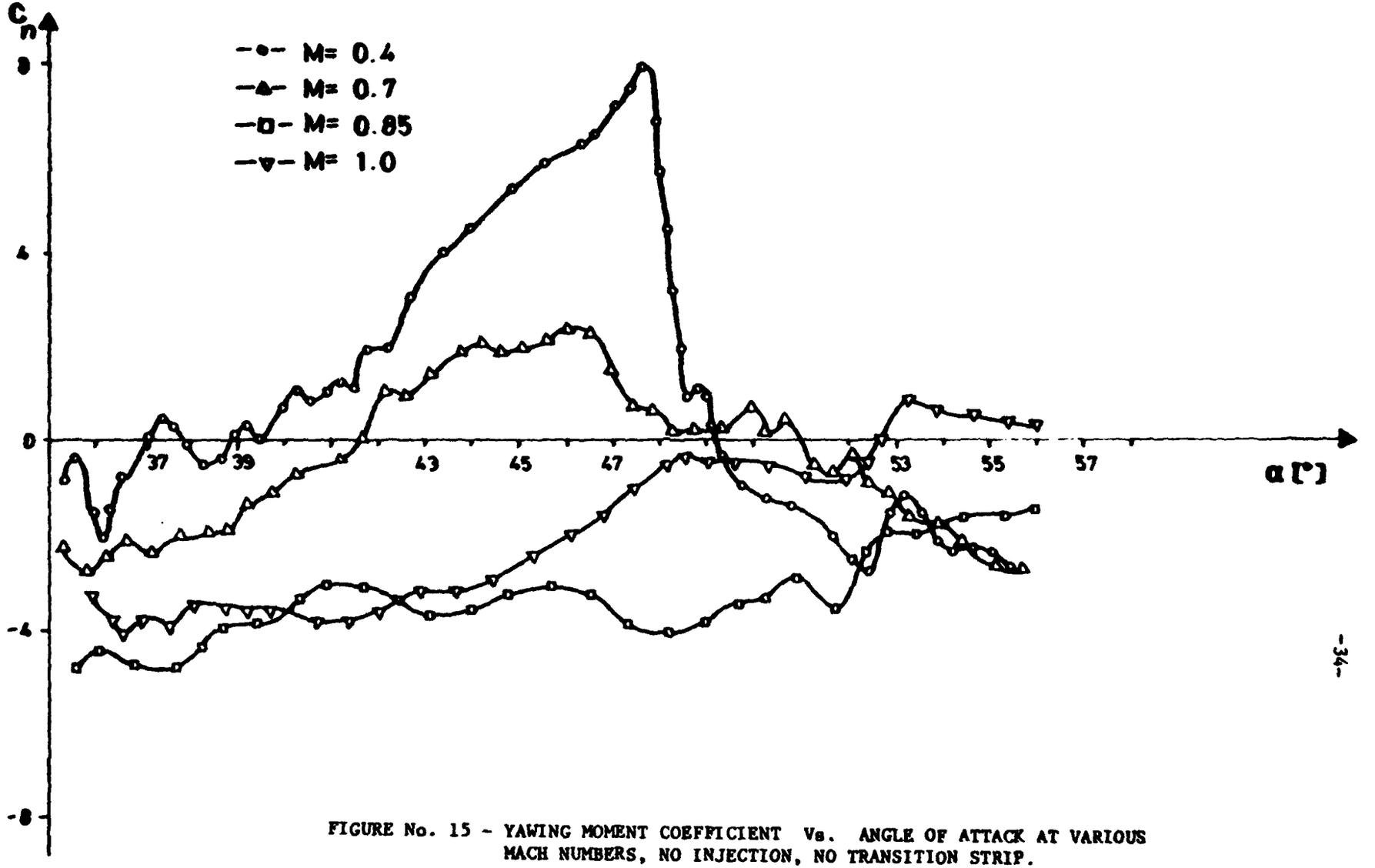

FIGURE No. 15 - YAWING MOMENT COEFFICIENT Vs. ANGLE OF ATTACK AT VARIOUS MACH NUMBERS, NO INJECTION, NO TRANSITION STRIP.

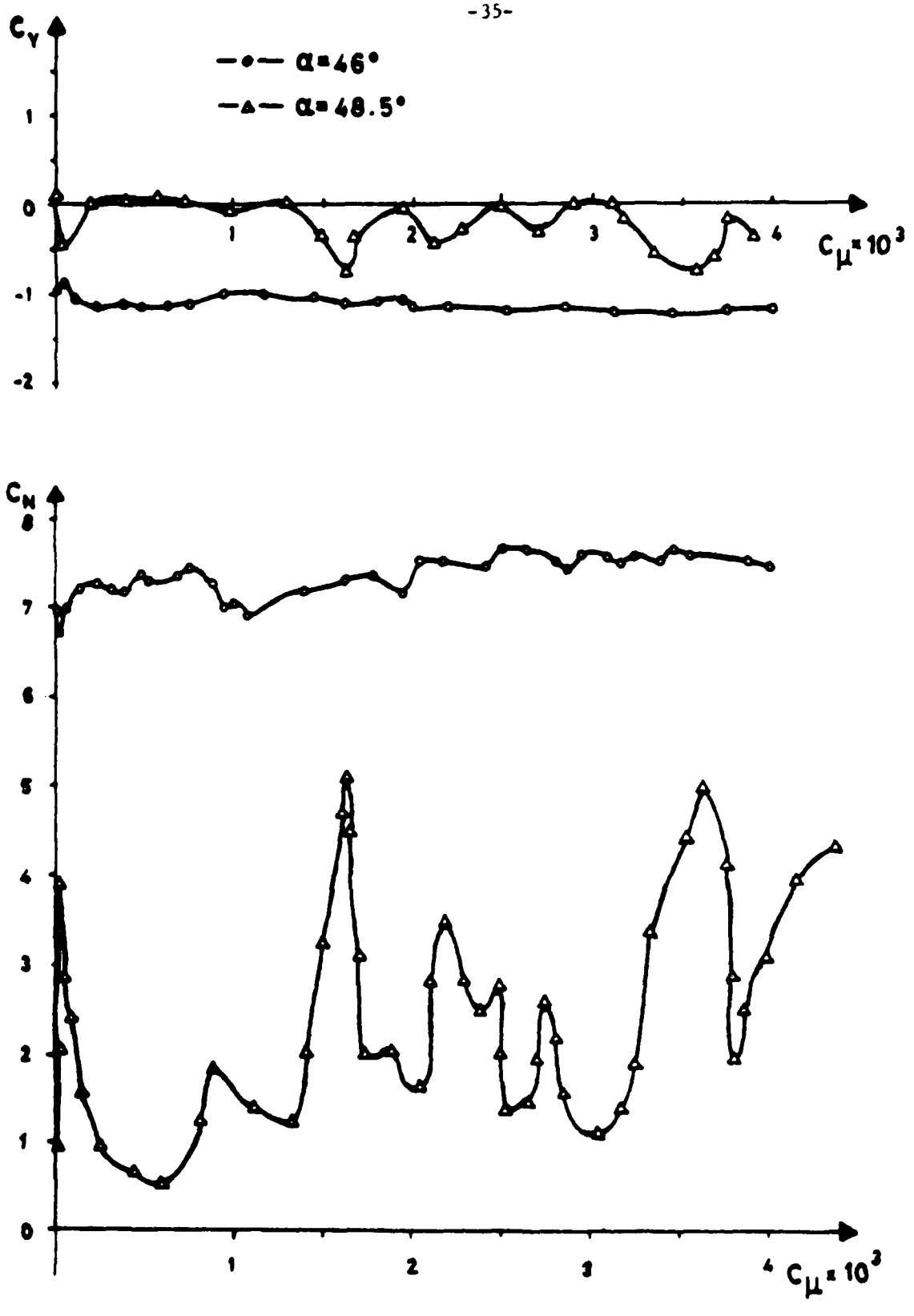

FIGURE No. 16 - SIDE FORCE AND YAWING MOMENT COEFFICIENTS Vs. BLOWING RATE COEFFICIENT AT M = 0.4, AT TWO ANGLES OF ATTACK, NO TRANSITION STRIP.

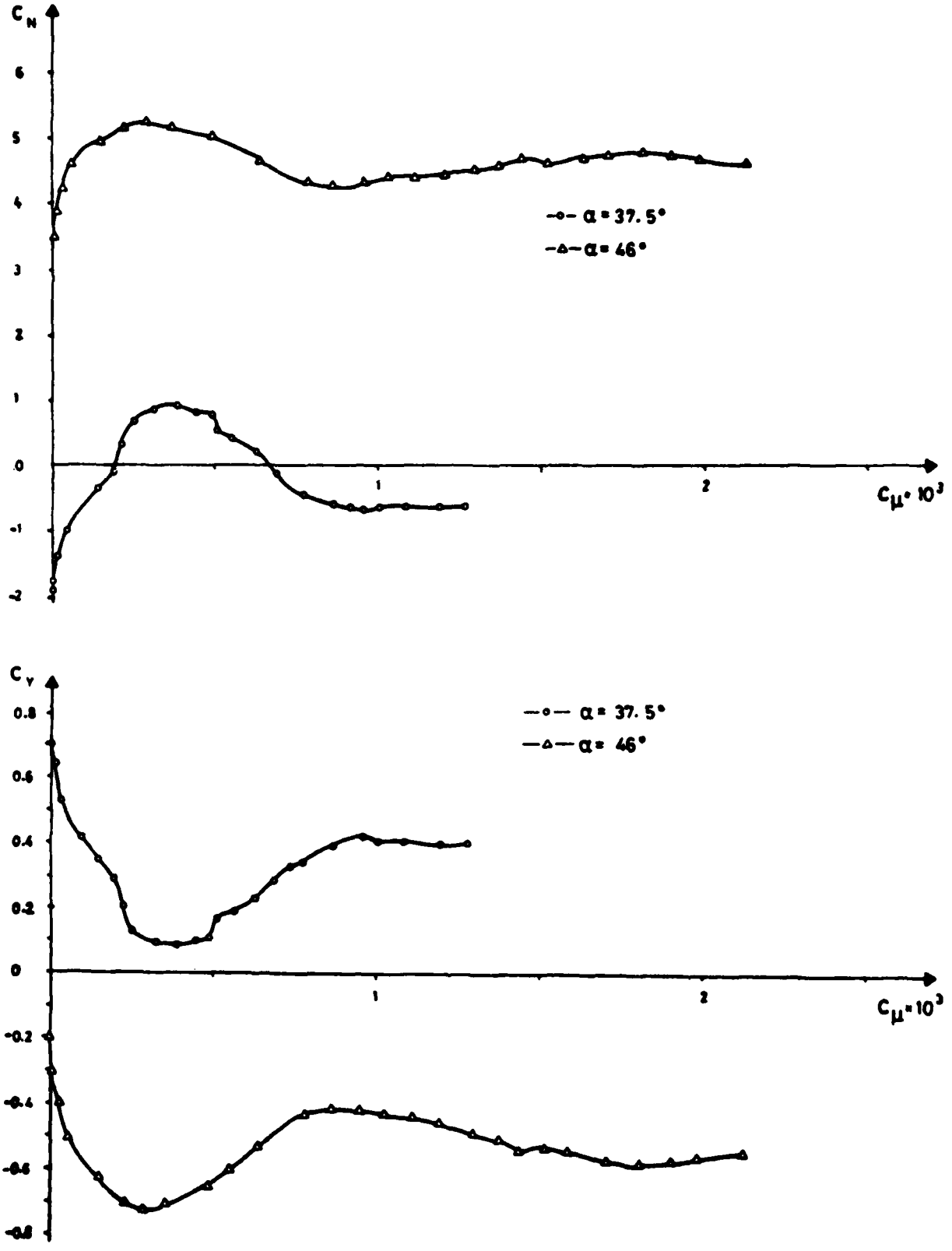

FIGURE No. 17 - SIDE FORCE AND YAWING MOMENT COEFFICIENTS Vs. BLOWING RATE COEFFICIENT AT M = 0.7, AT TWO ANGLES OF ATTACK.

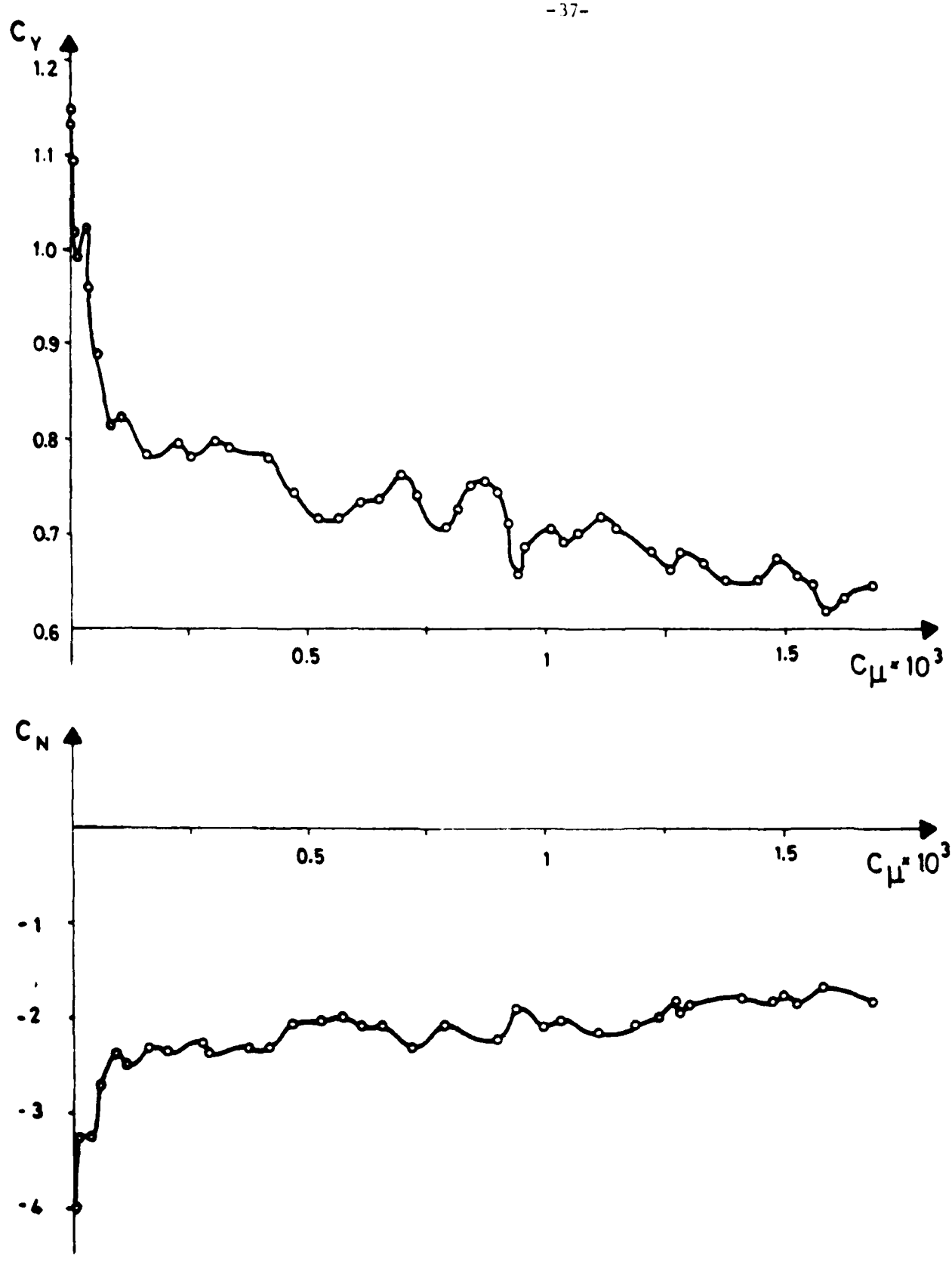

FIGURE No. 18 - SIDE FORCE AND YAWING MOMENT COEFFICIENTS Vs. BLOWING RATE COEFFICIENT AT M = 0.85, AT 47° ANGLE OF ATTACK.

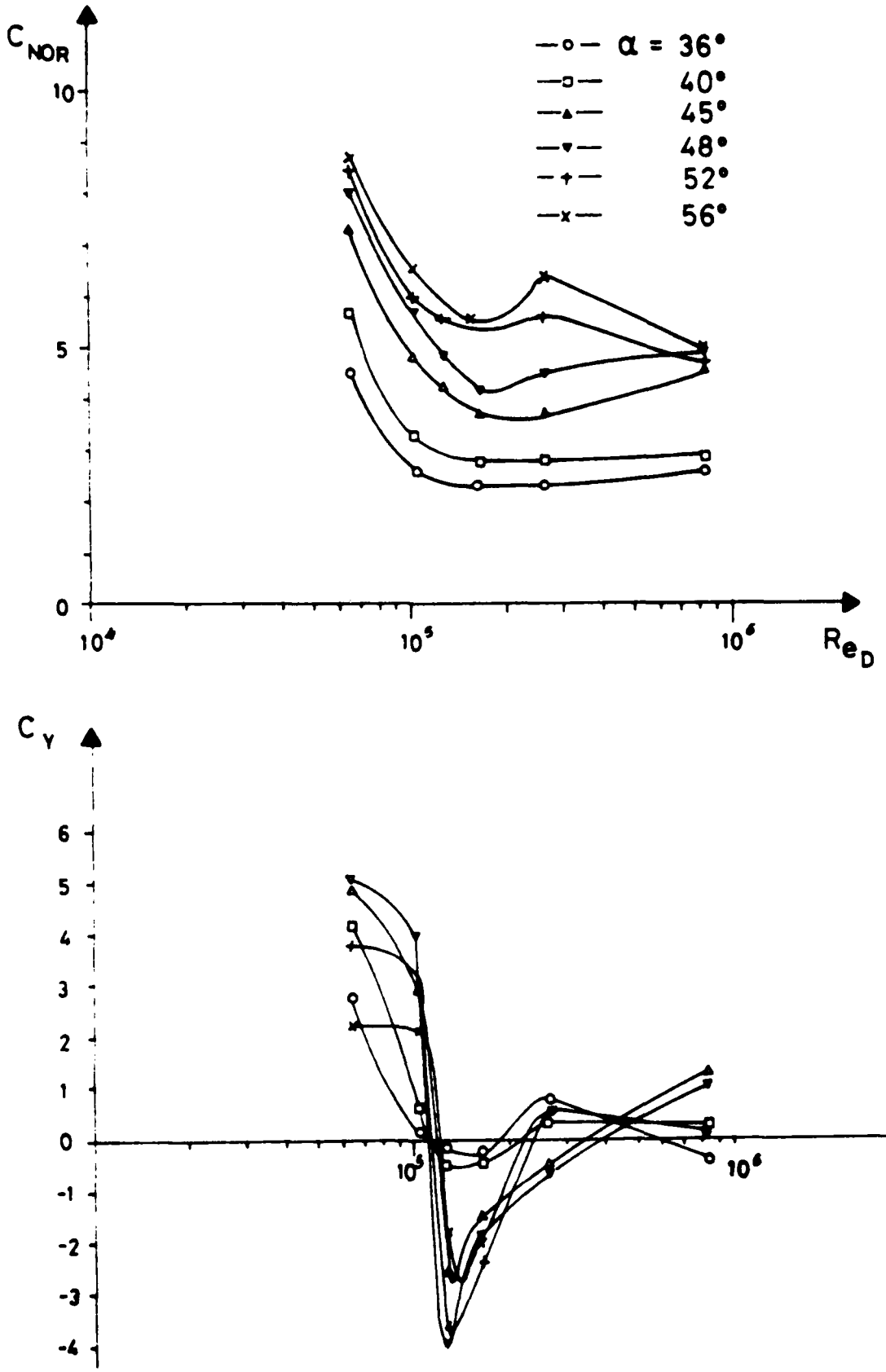

FIGURE No. 19 - NORMAL FORCE AND SIDE FORCE COEFFICIENTS Vs. REYNOLDS NUMBER, AT VARIOUS ANGLES OF ATTACK, NO TRANSITION STRIP, NO INJECTION.

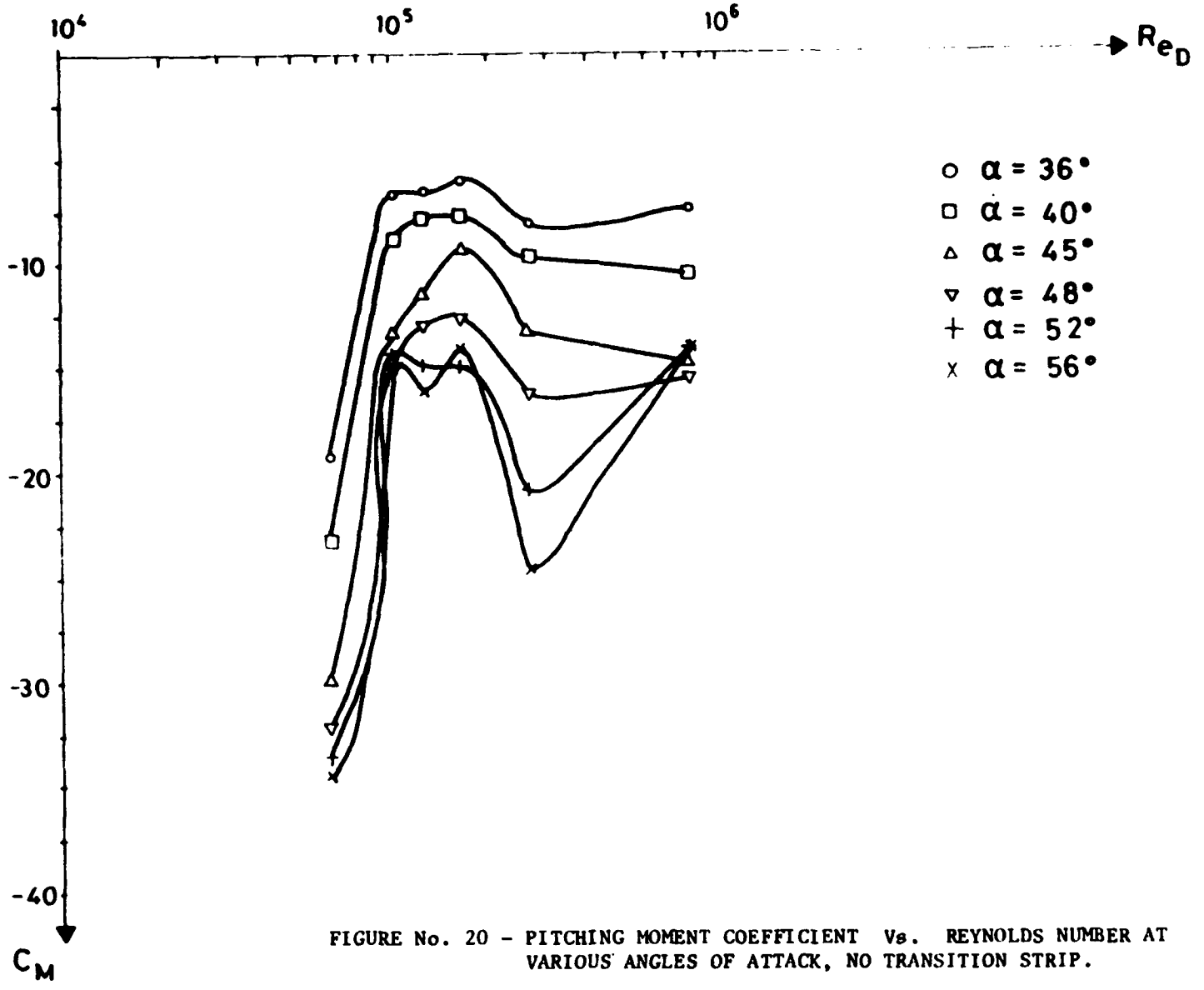

FIGURE No. 20 - PITCHING MOMENT COEFFICIENT Vs. REYNOLDS NUMBER AT VARIOUS ANGLES OF ATTACK, NO TRANSITION STRIP.

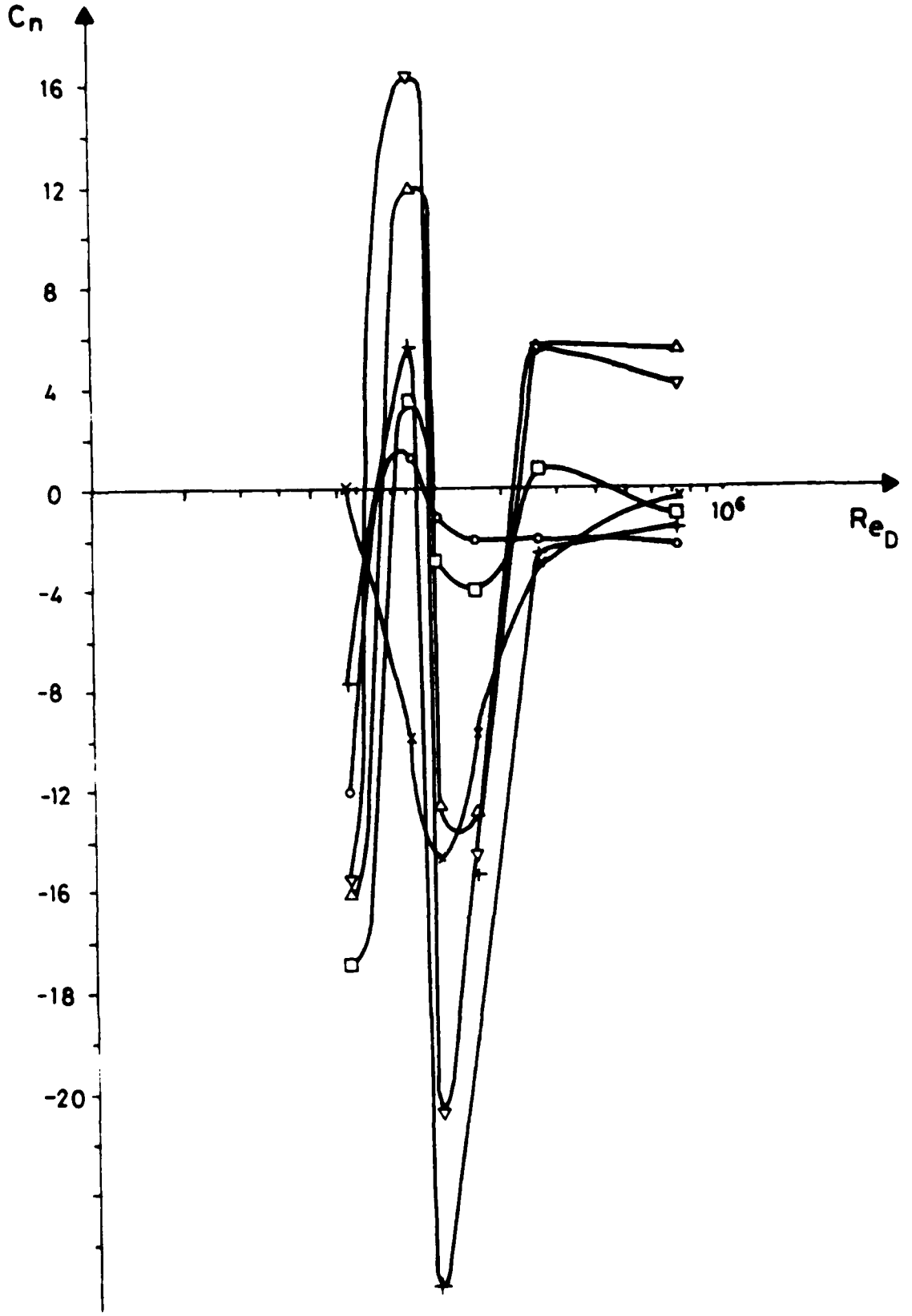

FIGURE No. 21 - YAWING MOMENT COEFFICIENT Vs. REYNOLDS NUMBER, AT VARIOUS ANGLES OF ATTACK, NO TRANSITION STRIP.

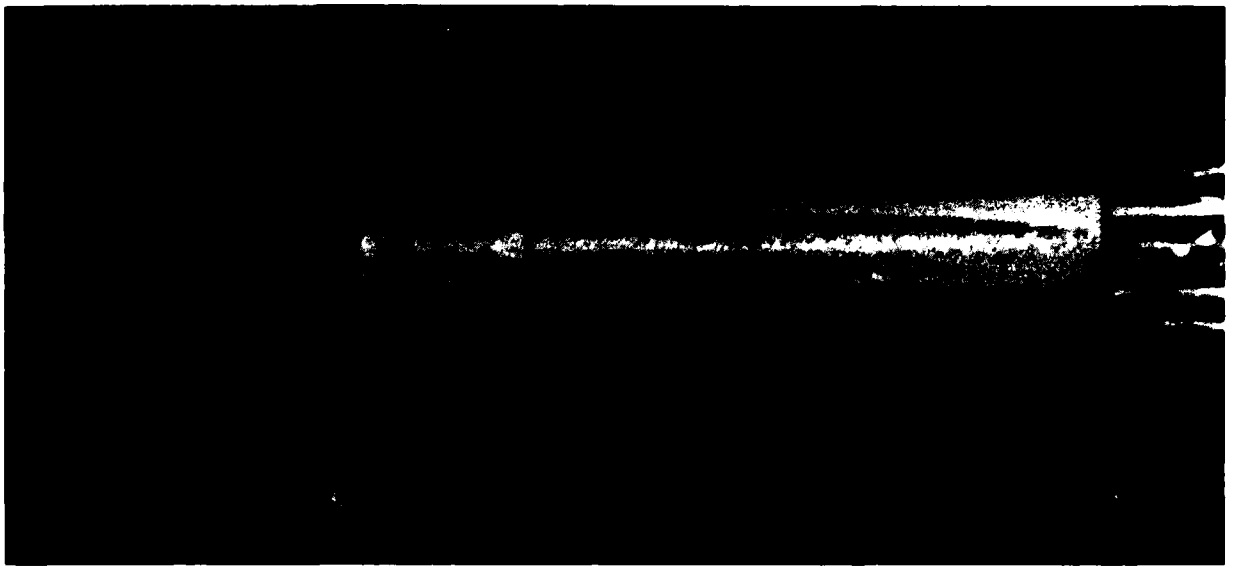

NO JET BLOWING

WITH JET BLOWING

FIGURE No. 22 - OIL FLOW VISUALIZATION OF THE CONE-CYLINDER MODEL AT V = 32 m/sec, $\alpha = 40^{\circ}$, WITH A TRANSITION RING AT x/D = 0.333.

NO JET BLOWING

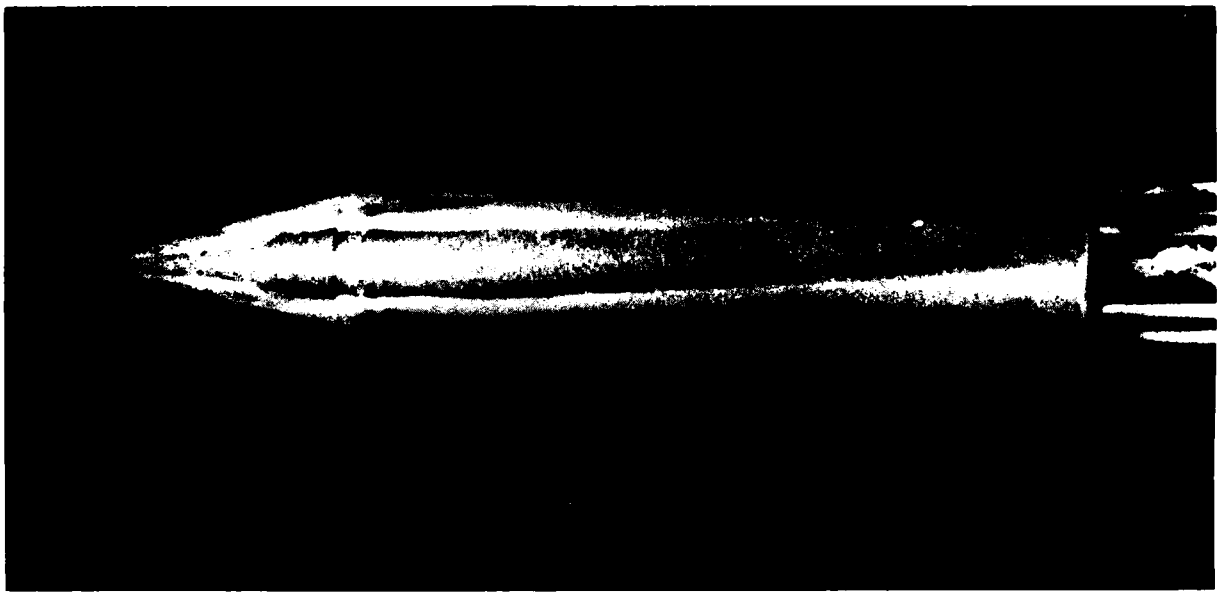

WITH JET BLOWING

FIGURE No. 23 - OIL FLOW VISUALIZATION OF THE CONE-CYLINDER MODEL AT V=32 m/sec, α = 55°, NO TRANSITION RING.

M = 0.46

M = 0.71

M = 0.87

M = 1.06

FIGURE No. 24 - SCHLIEREN PHOTOGRAPHS OF THE CONE-CYLINDER MODEL AT VARIOUS MACH NUMBERS, $\alpha = 47^{\circ}$, NO JET BLOWING.

NO JET BLOWING

WITH JET BLOWING

FIGURE No. 25 - SCHLIEREN PHOTOGRAPHS OF THE CONE CYLINDER MODEL AT **M = 0.7,** $\alpha = 37.5^{o}$.